PHILOSOPHICAL TRANSACTIONS OF THE ROYAL SOCIETY A MATHEMATICAL, PHYSICAL & ENGINEERING SCIENCES

Tidal Spectroscopy and Prediction

W. H. Munk and D. E. Cartwright

Phil. Trans. R. Soc. Lond. A 1966 **259**, doi: 10.1098/rsta.1966.0024, published 19 May 1966

TIDAL SPECTROSCOPY AND PREDICTION

By W. H. MUNK† and D. E. CARTWRIGHT‡

Institute of Geophysics and Planetary Physics, University of California, La Jolla

(*Communicated by Sir Edward Bullard, F.R.S.—Received* 21 *June* 1965)

CONTENTS

Nineteen years of hourly tide readings at Honolulu, Hawaii, and Newlyn, England, are analysed without astronomical prejudice as to what frequencies are present, and what are not, thus allowing for background noise. The method consists of generating various complex input functions $c_i(t)$ for the same time interval as the recorded tide $\zeta(t)$, and of determining the associated lag weights w in the convolutions

$$\hat{\zeta}(t) = \sum_i \sum_s w_{is} c_i(t-\tau_s) + \sum_{ij} \sum_{ss'} w_{ijss'} c_i(t-\tau_s)\, c_j(t-\tau_{s'}) + \ldots$$

by the condition $\langle(\zeta-\hat{\zeta})^2\rangle$ = minimum. The two expansions represent linear and bilinear processes; the Fourier transforms of w for any chosen i (or ij) are the linear (or bilinear) admittances.

† This work was started by W. H. M. at Churchill College, Cambridge University, with support of a Guggenheim Fellowship.

‡ On visit from the National Institute of Oceanography, U.K.

VOL. 259. A. 1105. (Price 18*s*.; U.S. $2.70) 64 [Published 19 May 1966

Input functions are the (time variable) spherical harmonics of the gravitational potential and of radiant flux on the Earth's surface; these functions are numerically generated hour by hour, directly from the Kepler–Newton laws and the known orbital constants of Moon and Sun, without time-harmonic expansions (unlike the harmonic method of Kelvin–Darwin–Doodson). The radiative input is required to predict non-gravitational tides, and it allows for the essential distinction that the Earth is opaque to radiation and transparent to gravitation.

The input functions are confined to bands, centred at 0, 1, 2, ... c/d, which occupy roughly one-fourth the frequency space (less for radiational inputs) at the -60 dB level. Within these bands the admittances turn out to be reasonably smooth, as expected. Subsequently we force the admittances to be smooth by truncating the expansion in s. Subject to this 'credo of smoothness' the overlapping gravitational, radiational and nonlinear admittances can be disentangled. The procedure consists of computing the lag weights by inverting a correlation matrix of input functions, and the admittances by subsequent Fourier inversion; the varying uncertainties in the tidal components are automatically allowed for. The residual record, $\zeta(t)-\hat{\zeta}(t)$, is associated with the irregular oscillations induced by winds and atmospheric pressure. The residual spectrum smoothly fills the space between the bands centred on 0, 1, 2, c/d and rises sharply toward 'zero' frequency, reflecting a similar pattern in the meteorological spectra. The residual spectrum rises into cusp-like peaks about each of the strong spectral lines, as might be expected from a low-frequency modulation of 'tidal carrier frequencies', but detailed analyses fail to confirm this hypothesis. Another feature is a slight 2 c/y 'jitter' in the admittances, probably the result of some trilinear interactions.

Once the ocean's *response* to various specified inputs has been determined for a given station, it can serve as a basis for a tide prediction which is perhaps more physical than the harmonic method now in use. The convolution formalism explicitly distinguishes between astronomic inputs and oceanographic response, with Kepler–Newtonian mechanics fully taken into account (in the harmonic method, K.–N. mechanics serves only to identify principal tidal frequencies). Moreover, the response method leads to a systematic expansion for weak nonlinearities. The response method gives better prediction with fewer station constants, but the improvement is small compared to the low frequency residuals. To reduce these we have tried a Wiener-type self prediction with past values of the recorded tide as input function. At Honolulu the residual variance can be reduced by 50 % for a prediction time of 40 days. At Newlyn where the effect of local weather (storm tides) is severe, the response method should be generalized to include as additional input functions some pertinent meteorological variables as well as sea level at other tide stations.

Notation

The following is a list of symbols frequently used in the text. Symbols used only in the Appendixes, or standard in tidal literature, are excluded.

g	mean gravitational acceleration at Earth's surface
θ, λ, t	geographical colatitude, East longitude, mean solar time
$V(\theta, \lambda; t)$	gravitational tide generating potential
$\zeta, \hat{\zeta}, \bar{\zeta}(t)$	observed, predicted, and lowpassed or 'mean' sea level
$\hat{\zeta}^{\mathrm{I}}, \hat{\zeta}^{\mathrm{II}}$	linear and bilinear predictors of sea level
$P_n^m(\mu)$	associated Legendre function of order m, degree n
$Y_n^m(\theta, \lambda) = U_n^m + \mathrm{i}V_n^m$	complex spherical harmonic (appendix A, equation (A 5))
$c_n^m(t) = a_n^m + \mathrm{i}b_n^m$	complex coefficient in spherical harmonic expansion of V/g (equation (2·11))
$\chi_n^m(t) = \alpha_n^m + \mathrm{i}\beta_n^m$	coefficient analogous to $c_n^m(t)$ for radiational potential
c_i, c	generalized forms of $c_n^m(t)$ or $\chi_n^m(t)$
$c^{m \pm m'}$	bilinear inputs derived from product of c^m and $c^{m'}$

$w_n^m(s) = u_n^m(s) + \mathrm{i}v_n^m(s)$	weights used in prediction formalism for $\hat{\zeta}(t)$ in terms of $c(t-\tau_s)$ (equation (2·12))
$w_i(s), w_{is}, w_s$	generalized notations for prediction weights
$\tau_s, \Delta\tau$	time lags used in argument of c or ζ; usually $\tau_s = s\Delta\tau$
Δt	sampling interval of time series
$\alpha(t), \xi(t)$	local zenith angle and parallax of Moon or Sun
c/d, c/m, c/y	cycles per day, month, year
f	frequency in c/d
f_n, k_n	basic tidal frequencies and their coefficients in harmonic tide development (§ 2*b*)
$G(f), H(f)$	complex amplitude spectra of $\zeta(t)$, and of $a_n^m(t)$ or $\alpha_n^m(t)$
$Z(f) = X + \mathrm{i}Y$	complex linear admittance of $\zeta(t)$ to $c(t)$
G_r, H_r, Z_r, X_r, Y_r	filtered estimators of $G(f)$, $H(f)$, $Z(f)$ at $f = r/355$
γ_r^2	estimate of coherency at $f = r/355$ (equation (4·11))
E_r^i, E_r^o, C_r, Q_r	'energy' or 'variance' spectra of input (such as $a(t)$) and output (such as $\zeta(t)$), and their co- and quadrature spectra
σ^2	variance of $(\zeta - \hat{\zeta})$
σ_m^2	variance of ζ less variance of $(\zeta - \hat{\zeta}_m)$, where $\hat{\zeta}_m$ is the prediction for species m (equation (4·20))
$\langle\ \rangle$	average over time, or over consecutive spectral frequencies.

1. Introduction

Since the days of George Darwin, tide records have been analysed for the amplitude and phase at those particular periods (and their harmonics), which had been previously observed in the orbital motion of the Moon and Sun. The assumption was implicit that tide records could be accounted for to any desired degree of precision if only a sufficient number of such periods were included. In the language of 'stationary time series' this is equivalent to the assertion that the tidal *line spectrum* exists all by itself, rather than being superimposed on a *continuum* (or 'noisy' spectrum). But noise-free processes do not occur (except in the literature on tidal phenomena).

In tide records the continuum is associated largely with irregular oscillations due to wind and pressure. By 1960 the continuum had been successfully measured from the high frequencies associated with sea and swell down to frequencies as low as 8 c/d (cycles per day), only two octaves removed from the semidiurnal tides (2 c/d). The spectrum was found to rise with decreasing frequency; extrapolation into tidal frequencies suggested that if one were to analyse tide records without preconceived ideas as to what periods were present and what periods were not, then one would obtain just about as much mean-square amplitude at nontidal periods as had been found for some of the weaker spectral lines. This suggestion has now been confirmed. It means that the weaker lines are hopelessly contaminated by noise, and this accounts for some of the inconsistencies from one year to the next.

We decided to take a new look at the tide records, without astronomical prejudice and freely allowing for the presence of noise. Modern methods of time series analysis seemed appropriate. Experimental analyses with very long series are readily carried out with high-speed computers. Continuous hourly readings for half a century or longer are available for

more than a dozen ports (comprising some 10^7 observations) and constitute a unique geophysical record.

As a result of our analyses we are led to propose a method of tide prediction which differs somewhat from the classical method now universally accepted. The proposed method leads to slightly greater precision with a lesser number of tidal constants; there are other advantages. It can be said that we are here attempting to improve the one geophysical prediction that works tolerably well already; to this charge we plead guilty. But predicting and learning are in a sense orthogonal, and the most interesting effects are those that cause most trouble with forecasting: the continuum, the nongravitational tides, and the nonlinear interactions. Nearly all of the tidal energy is in narrow clusters centred at frequencies of 0, 1 and 2 c/d. For prediction this is of great advantage. For exploration one would have preferred a broad band excitation, such as tidal forces arising from a nearby supernova.

2. Concerning tide prediction

(*a*) *Nonharmonic method*

The connexion between Moon and tides is so obvious that long before the formulation of any theory quite satisfactory rule-of-thumb predictions of tide were made and published. Tide tables constructed by undivulged methods were considered as gainful family possessions and passed on from father to son. The Liverpool Tide Tables published by a clergyman named Holden carried this to its highest perfection.

Starting 1831, Sir John Lubbock initiated what has been called the *nonharmonic* method of tide prediction. Tides at a given port are represented by certain tidal elements: time and height of high water, low water. These are related to astronomical observables: the age of the Moon (reckoned from new Moon), the declination, and the parallax of Moon and Sun. The prediction is made by successive approximations. For example,

height of high water
= mean height above datum + correction for age + correction for declination
+ correction for parallax + diurnal inequality.

The corrections were derived by successive regressions between observed tidal and orbital elements using long series of data. Tables produced in this manner were quite successful for ports with predominantly semidiurnal tides (as in England). According to Whewell (1837) 'Some mistakes in these as first published (mistakes unimportant as to the theoretical value of the work) served to show the jealousy of the practical tide table calculators, by the acrimony with which the oversights were dwelt upon; but in a very few years, the tables thus produced by an open and scientific process were more exact than those which resulted from any of the secrets; and thus practice was brought into its proper subordination to theory.'

(*b*) *Harmonic method*

The *harmonic* method of tide analysis was developed by Lord Kelvin and Sir George Darwin starting 1867, following an earlier suggestion by Laplace along similar lines. The tidal elevation at a given port is predicted according to

$$\zeta(t) = \sum_{\mathbf{k}} C_{\mathbf{k}} \cos(2\pi \mathbf{k}.\mathbf{f}t + \theta_{\mathbf{k}}), \qquad (2{\cdot}1)$$

summed over a set of denumerable frequencies

$$\mathbf{k}.\mathbf{f} = k_1 f_1 + k_2 f_2 + \ldots + k_6 f_6 \quad (k = 0, \pm 1, \pm 2. \ldots), \tag{2·2}$$

where f is a six-dimensional vector whose components are the basic frequencies in the motion of Earth, Moon, and Sun; namely:

$f_1^{-1} = 1$ day is the period of the Earth's rotation (relative to Sun),
$f_2^{-1} = 1$ month is the period of the Moon's orbital motion,
$f_3^{-1} = 1$ year is the period of the Sun's orbital motion,
$f_4^{-1} \approx 8{\cdot}85$ years is the period of lunar perigee,
$f_5^{-1} \approx 18{\cdot}61$ years is the period of regression of lunar nodes,
$f_6^{-1} \approx 20\,900$ years is the period of solar perigee.

The coefficients $C_{\mathbf{k}}, \theta_{\mathbf{k}}$ are found by harmonic analysis of the tide record $\zeta(t)$ for frequencies (2·2) specified in advance (to eight significant figures) on the basis of the astronomical observations.

The 'integer vector' $\mathbf{k} = (k_1\ k_2\ k_3\ k_4\ k_5\ k_6)$

completely defines the frequency $\mathbf{k}.\mathbf{f}$. Because of the predominant effect of the Moon, there is some convenience in referring to a lunar day of $1/f_1^{\leftmoon} = 1{\cdot}035$ solar days, the relation being $f_1^{\leftmoon} = f_1^{\odot} - f_2 + f_3$. The resulting set

$$(k_1\ k_2\ k_3\ k_4\ k_5\ k_6)_{\leftmoon} = (k_1\ k_2 + k_1\ k_3 - k_1\ k_4\ k_5\ k_6)_{\odot} \tag{2·3}$$

will be called the 'Doodson number'.† $k_1 = 0, 1, 2$ refers to frequencies near 0, 1, 2 c/ld (cycles per lunar day), the long period, diurnal and semidiurnal *species*, respectively. $(k_1\ k_2)$ is called the *group* number, and $(k_1\ k_2\ k_3)$ the *constituent* number. Neighbouring groups differ in frequency by 1 c/m (cycle per month); neighbouring constituents by 1 c/y (cycle per year). In the language of spectroscopy the tidal spectra show four orders of splitting: monthly splitting, a fine structure due to yearly splitting, a hyperfine structure from lunar perigee and regressional splitting, and a further splitting associated with solar perigee.

In principle, prediction by the harmonic method could be performed without any recourse to Keplerian and Newtonian mechanics, without regard even as to whether any given term is lunar or solar. All that needs to be done is to analyse a long record into all possible Doodson numbers, starting with zero k values and proceeding until the computed amplitudes are below some desired limit. For a limiting amplitude of 10^{-4} times the largest term, about 400 terms are required, and in no instance does $|k|$ exceed 6.

But this is not a practical procedure. The largest terms are chosen once and for all on the basis of potential theory. If the sea surface coincided with a potential surface, the departure from mean sea level (the equilibrium height) would be given by

$$\frac{V}{g} = \frac{GM}{g\rho} - \frac{V_0}{g}, \tag{2·4}$$

where $V(t)$ is the gravitational potential due to the Moon or Sun (mass M) whose centre of mass is at a distance $\rho(t)$ from the point of observation P, G is the gravitational constant, g local gravity, and V_0 a suitable reference potential. Let a designate the Earth's radius, $R(t)$

† Doodson (1921) uses $(k_1\ k_2 + 5\ k_3 + 5\ k_4 + 5\ k_5 + 5\ k_6 + 5)_{\leftmoon}$ to assure positive indices.

the distance between the centres of Earth and M, and $\xi(t) = a/R$ the parallax. Then (see appendix A)

$$\rho = R(1+\xi^2-2\xi\cos\alpha)^{\frac{1}{2}}, \tag{2·5}$$

where $\alpha(t)$ is the local zenith angle of M. For any point P

$$\alpha = \alpha(Z, L), \tag{2·6}$$

where $Z(t)$ is the polar angle, and $L(t)$ the (terrestrial) longitude of M. The distance, polar angle and longitude of M can now be expressed in terms of sines and cosines of six fundamental arguments,

$$R_{\leftmoon}, R_{\leftmoon}, L_{\leftmoon}, R_{\odot}, Z_{\odot}, L_{\odot} = \text{functions of } (2\pi t^h/24^h, h_{\leftmoon}, h_{\odot}, p_{\leftmoon}, n_{\leftmoon}, p_{\odot}), \tag{2·7}$$

whose frequencies are the components of $\mathbf{f}$ in equation (2). Here t is Greenwich time, $h_{\leftmoon}$ and $h_{\odot}$ are the mean ecliptic longitudes, $p_{\leftmoon}$ and $p_{\odot}$ the longitudes of perigee, and $n_{\leftmoon}$ the longitude of the Moon's nodes.† The arguments $h_{\leftmoon}, h_{\odot}, \ldots, p_{\odot}$ are usually given in the form

$$A+BT+CT^2, \tag{2·8}$$

where T is in Julian centuries since 1 January 1900, A is the phase at $T = 0$, $B = 2\pi f$ denotes the frequency in cycles per century, and CT^2 is a small correction arising from planetary perturbations and tidal friction.

A systematic development of equations (4) to (8) leads to the trigonometric expansion

$$V/g = \sum_{\mathbf{k}} \tilde{C}_{\mathbf{k}} \cos(2\pi \mathbf{k}.\mathbf{f}t + \tilde{\theta}_{\mathbf{k}}),$$

which associates any Doodson number $\mathbf{k}$ with an amplitude $\tilde{C}_{\mathbf{k}}$ and phase $\tilde{\theta}_{\mathbf{k}}$ consistent with potential theory. In this way the frequencies of the important terms are selected.

Darwin considered $p_{\leftmoon}, n_{\leftmoon}, p_{\odot}$ as sensibly constant over any one year, and expanded in terms of t, $h_{\leftmoon}$, $h_{\odot}$ only; the frequencies are then fully defined by the constituent numbers $(k_1 k_2 k_3)$. Darwin's expansion included 39 terms, none smaller than 10^{-3} of the largest amplitude, and all within the limits $|k| \leqslant 3$. This development was generally accepted by 1883, and led to substantial improvements over Lubbock's method. But it was found that when all Darwinian constituents were removed, the residual tides still showed significant components. Consequently Doodson carried out the expansion into some 400 terms exceeding 10^{-4} of the amplitude of the largest term and associating each term with the complete Doodson number.

In the application of the harmonic method one encounters an awkward situation which is not corrected by the more complete expansion of Doodson's. At most tide stations records are available for only a few years or less, and it is not practical‡ to resolve terms whose frequencies differ by less than 1 c/y. We are back to constituents $(k_1 k_2 k_3)$ of the Darwin type. The accepted procedure is to replace equation (1) by

$$\hat{\zeta}(t) = \sum_{\mathbf{k}} f_{\mathbf{k}} C_{\mathbf{k}} \cos(2\pi \mathbf{k}.\mathbf{f}t + \theta_{\mathbf{k}} + u_{\mathbf{k}}), \tag{2·9}$$

† The classical notation for $h_{\leftmoon}$, $h_{\odot}$, $p_{\leftmoon}$, $n_{\leftmoon}$, $p_{\odot}$ is s, h, p, n, q.

‡ But Doodson's statement that 19 years of record are required to separate regressional terms is incomplete. Any four known values of $\zeta(t)$ will provide four equations to solve for the amplitudes and phases $C_1, \theta_1, C_2, \theta_2$ at frequencies f_1, f_2, regardless of the frequency separation. In an ideal record, 4-hourly values could resolve regressional splitting! A statement concerning the required length of record has to take into account the underlying noise spectrum and, when this is done, the situation is not much better than stated by Doodson (Munk & Hasselmann 1964).

where the factors $f_k(t)$, $u_k(t)$ are taken as constant over any one year, but vary from year to year, principally with the nodal period of 18·61 y. The f, u factors were introduced by Darwin and are tabulated in manuals on tide prediction. The 21 000 y variation (frequency f_6) is ignored. The use of slowly varying amplitudes and phases implies that the Darwin–Doodson method is not, strictly speaking, a harmonic method.

At European ports and elsewhere the distortion of the tides by shallow water effects cannot be ignored. This situation has been met in various ways. Following the suggestion of Ferrel and Darwin, one can introduce further constituents whose frequencies are the sums and differences of the important 'linear constituents'. For some ports the number of required shallow water consituents becomes unmanageable. In England, Doodson (1947) then examines by further harmonic analysis the residual between observed and predicted tides, with as many shallow water constituents included as is possible. In Germany, Horn (1948, 1960) has introduced a 'folding scheme' (Appendix C) and in Holland one relies on a nonharmonic method.

(c) *Response method*

The complexity of the Darwin–Doodson expansion is, in a sense, an artifice arising from an insistence of expressing the tides as sums of harmonic functions of time. With h, p, n as given functions of time, it is nowadays relatively simple to evaluate equations (4) to (8) numerically and obtain a computer-generated time series $V(t)$. Suppose that hourly values $V(t)$ have been computed for a given port. One could attempt a prediction for time t as a weighed sum of past and present values of the potential,

$$\hat{\zeta}(t) = \sum_s w(s)\, V(t-\tau_s), \tag{2·10}$$

with the weights w determined so that the prediction error $\zeta(t)-\hat{\zeta}(t)$ is a minimum in the least-square sense. The weights have a simple physical interpretation: they represent the sea level *response* at the port to a unit impulse $V(t) = \delta(t)$, hence the name 'response method'. The actual input function $V(t)$ may be regarded as a sequence of such impulses.

The formulation (10) has the defect that it assumes predictions for any port to depend only on the equilibrium tide at this port. One would do better to evaluate the equilibrium tide at a grid of points surrounding the port, thus obtaining $V_1(t), V_2(t), \ldots$, and then predicting according to

$$\hat{\zeta}(t) = \sum_s w_1(s)\, V_1(t-\tau_s) + \sum_s w_2(s)\, V_2(t-\tau_s) + \ldots.$$

Alternatively one could expand $V(t)$ in the vicinity of the port (position θ_0, λ_0) in terms of a Taylor series

$$V + (\theta-\theta_0)\, V_\theta + (\lambda-\lambda_0)\, V_\lambda + \ldots,$$

numerically evaluate $V(t)$ and its spatial derivatives $V_\theta, V_\lambda, \ldots$ at position θ_0, λ_0, and attempt a prediction according to

$$\hat{\zeta}(t) = \sum_s w_1(s)\, V(t-\tau_s) + \sum_s w_2(s)\, V_\theta(t-\tau_s) + \sum w_3(s)\, V_\lambda(t-\tau_s) + \ldots.$$

Our scheme is to expand $V(t)$ in spherical harmonics,

$$V(\theta, \lambda; t) = g \sum_{n=0}^{n} \sum_{m=0}^{n} [a_n^m(t)\, U_n^m(\theta, \lambda) + b_n^m(t)\, V_n^m(\theta, \lambda)], \tag{2·11}$$

and compute the coefficients $a_n^m(t)$ and $b_n^m(t)$ for the desired time interval. The convergence of the spherical harmonics is rapid and just a few terms m, n will do. The m-values separate input functions according to species. The prediction formalism is then†

$$\hat{\zeta}(t) = \sum_{m,n} \sum_{s} [u_n^m(s)\, a_n^m(t-\tau_s) + v_n^m(s)\, b_n^m(t-\tau_s)]. \tag{2·12}$$

The prediction weights $w_n^m(s) = u_n^m(s) + iv_n^m(s)$ are determined by least-square methods, and tabulated for each port (these take the place of the tabulated coefficients C_k, θ_k in the harmonic method). For each year the global tide function $c_n^m(t) = a_n^m(t) + ib_n^m(t)$ is computed and the tides then predicted by forming weighted sums of c using the weights w appropriate to each port. The spectra of the numerically generated time series $c(t)$ have all the complexity of the Darwin–Doodson expansion; but there is no need for carrying out this expansion, as the series $c(t)$ serves as direct input into the convolution prediction. There is no need to set a lower bound on spectral lines; all lines are taken into account in an optimum sense. There is no need for the f, u factors, for the nodal variation (and even the 21 000 y variation) is already built into $c(t)$. In this way the response method makes explicit and general what the harmonic method does anyway—in the process of applying the f, u factors. The response method leads to a more systematic procedure, better adapted to computer use. Its formalism is readily extended (as we shall see) to include nonlinear, and perhaps even meteorological effects.

The harmonic and response methods are closely related. As the lower bound on spectral lines is reduced, and as the number of spherical harmonics and lags are increased, the results of the two methods rapidly approach one another. It should be stated at the outset that under ordinary circumstances the improvement in the accuracy of tide prediction by the use of the response method is slight. But there is an advantage in introducing Kepler–Newtonian mechanics from the very start, and the prediction formalism (12) makes the separation of astronomy from oceanography more explicit than does equation (1). In the sense that the response method does not involve a time-harmonic expansion (it involves only a spherical-harmonic expansion), it is a move back toward the nonharmonic method of Lubbock.

3. Input functions

We have written a computer program for generating the coefficients $c_n^m(t)$ arising from lunar gravitational, solar gravitational, and radiational effects, for any specified values of m, n, and for any prescribed start time, time interval and end time. The numerical scheme follows a series of steps already outlined in equations (2·4) to (2·8). The derivation of the gravitational potential does not differ much from that given by Doodson (or for that matter by Darwin), but there are some innovations. The normalization of spherical harmonics is adapted from quantum mechanics, as this leads to the most symmetrical expressions for $c_n^m(t)$. We have included some third-order terms in the lunar eccentricity, and allowed for planetary perturbations of the solar eccentricity. Numerical values concerning the Sun–Moon–Earth system have been revised. Details are found in the appendix.

† Laplace attempted to predict the tides at Brest by convolutions upon major terms with *single* weighted lags. The poor results so obtained led him to propose a harmonic method.

The use of the convolution method carries some obligation to include a complete set of realistic input functions. We must do something about such features in the tide records that cannot be accounted for by the gravitational tide-producing forces.

For example, sea level responds to surface pressure associated with atmospheric tides. At temperate latitudes, maximum pressure occurs around 10 a.m. and 10 p.m. local time, minimum pressure at 4 a.m. and 4 p.m., with amplitudes of the order of 1 mb (gravitational forces on the atmosphere can account for only 1 % of this variation). There are also irregular day-to-day pressure fluctuation, possibly by many millibars, associated with 'weather'. In the former case we have a process with a *discrete* (or line) spectrum whose frequencies overlap the gravitational line spectrum. In the latter case the process has a *continuous* (or noisy) spectrum which underlies the discrete spectrum. Similarly, the land-and-sea breeze régime is associated with a line spectrum, principally at 1 and 2 c/d, as well as a continuum. Storm tides are an extreme case of the latter type.

September sea level typically exceeds March sea level by 20 cm in the northern hemisphere; the reverse holds in the southern hemisphere (Patullo, Munk, Revelle & Strong 1955). Tidal effects and atmospheric pressure effects can only account for 10 % of the seasonal oscillation. Local changes in the specific volume of the water associated with water transport, solar radiation, back radiation, evaporation, etc., appear to be responsible. The total *mass* of the water column plus air column remains sensibly constant, so that a pressure recorder on the sea bottom would hardly sense the seasonal fluctuation in sea level. In addition, there are irregular variations from year to year. Again we may refer to the discrete spectrum (principally at 1 and 2 c/y) and the continuum.

We distinguish between three input functions, with the following spectral properties:

(i) The known gravitational line spectrum (lunar and solar).
(ii) The unknown nongravitational line spectrum.
(iii) The unknown nongravitational continuum.

(ii) and (iii) are ultimately the result of radiational processes, but at different stages of 'orderliness'. In a highly dissipative atmosphere strongly coupled by nonlinear processes, the line spectrum arising from the daily and seasonal variation in solar radiation is no longer discernible in the 'weather' and in the long-term variations. The prediction problem associated with (iii) will require special consideration.

We need an input function to model (ii). The function must, in some vital way, be related to the daily pressure and wind variations and to the seasonal changes in ocean temperature, and yet avoid the need for detailed solution of these complicated processes. For a trial input we define the radiational function

$$\begin{aligned}\mathscr{R} &= S(\bar{R}_\odot/\rho_\odot)\cos\alpha \text{ in day-time} \quad (0\leqslant\alpha\leqslant\tfrac{1}{2}\pi),\\ &= 0 \text{ in night-time} \quad (\tfrac{1}{2}\pi\leqslant\alpha\leqslant\pi),\end{aligned}$$

which varies with the radiant energy falling on a unit surface in a unit time. Expansion in spherical harmonics (appendix A) gives

$$\frac{\mathscr{R}}{S}=\frac{\bar{R}_\odot}{R_\odot}\left\{\tfrac{1}{2}\mu+\sum_{n=2,4,\ldots}\frac{2n+1}{2}\left[\frac{(1)\,(-1)\ldots(3-n)}{(2)\,(4)\ldots(2+n)}\right]P_n(\mu)\right\},$$

where $R_\odot$ and $P_n(\mu)$ can now be expressed in terms of the fundamental orbital constants, just as was done for the gravitational potential

$$\frac{V}{g} = a\frac{M_\odot}{M_\oplus}\sum_{n=2,\,3,\ldots}\bar{\xi}^{n+1}\left(\frac{\bar{R}_\odot}{\bar{R}_\odot}\right)^{n+1}P_n(\mu).$$

The essential distinction between gravitational and radiational inputs is that the Earth is transparent to gravity and opaque to radiation, and this is contained in the formulation of the input functions. The 'clipped' day and night distribution of the radiation function is much richer in higher harmonics than the gravitation function, as observed. One may hope that the seasonal modulation of the daily pressures and winds is properly modelled by the radiation function, so that the fine structure in the input spectra near 1, 2, ..., c/d is in the proper proportion.

4. Linear analysis

(a) *The physical system*

Before analysing an actual record of sea level, we must first outline the main physical concepts involved in a linear régime, and the corresponding processes required to analyse them. Nonlinear perturbations will be considered in § 7. We concentrate attention on the coefficients $a_n^m(t)$, $b_n^m(t)$ of the gravitational potential $V(\theta, \lambda; t)$ (equation (2·11)). The complex input potential and the recorded tide can be represented, for any m, n, by

$$G(f) = \int_{-\infty}^{\infty} c(t)\,\mathrm{e}^{2\pi i f t}\,\mathrm{d}t, \quad H(f) = \int_{-\infty}^{\infty} \zeta(t)\,\mathrm{e}^{2\pi i f t}\,\mathrm{d}t, \tag{4·1}$$

respectively. The same quantities are involved in the 'impulse response' relation,

$$\zeta(t) = \text{real part of} \int_0^{\infty} c^*(t-\tau)\,w(\tau)\,\mathrm{d}\tau, \tag{4·2}$$

where $c^* = a - ib$ is the complex conjugate of c, and $w(t) = u(t) + iv(t)$ is the sea-level response following an instantaneous value c^* at time $t = 0$. The Fourier transform of the impulse response is the 'admittance'

$$Z(f) = \int_0^{\infty} w(\tau)\,\mathrm{e}^{-2\pi i f \tau}\,\mathrm{d}\tau = H(f)/G(f), \tag{4·3, 4·4}$$

embodying an 'amplitude response' $|Z(f)|$ and a phase lead $\arg Z(f)$. Relations analogous to (4·1)–(4·4) are fundamental to a wide variety of linear noise-free physical systems.

A common approach is to estimate values of $G(f)$ and $H(f)$ at appropriate frequencies by spectral analysis of $c(t)$ and $\zeta(t)$ respectively, and then form $Z(f) = H(f)/G(f)$. This method suffers from neglect of the 'noise' which is inevitably present in H. In that event (4·4) is no longer a valid definition of Z. An estimate of Z is obtained by (4·3), or by cross-spectral analysis.

(b) *Noise-free estimates for discrete sampling*

For sampling at discrete intervals, spectral estimates G_r, H_r of $a_n^m(t)$ and $\zeta(t)$ were formed according to

$$\left.\begin{aligned} G_r &= 2n^{-1}\sum_t \Psi(t)\,a(t)\exp(2\pi i r t/355), \\ H_r &= 2n^{-1}\sum_t \Psi(t)\,\zeta(t)\exp(2\pi i r t/355), \end{aligned}\right\} \tag{4·5}$$

where the summations is from $t = -355d$ to $+355d$ at intervals Δt, $n = 710/\Delta t$, and $\Psi(t)$ is the 'cosine-taper' function $1+\cos(\pi t/355)$, inserted for rapid convergence of 'side-band' effects. In most cases $a(t)$ and $\zeta(t)$ have both previously been 'smoothed' by a low-pass filter with cutoff at 4 c/d, so that 3 h values ($\Delta t = \frac{1}{8}$ day, $n = 2840$) are used in (4·5) without trouble from 'aliasing'. The period of 355 days is close to 13 lunar months and to 1 year, so that all the tidal constituents fall centrally within the filters corresponding to integral values of r (Cartwright & Catton 1963). Note that the spectrum of $b(t)$ is not required, since it is identical with the spectrum of $a(t)$ with a phase change of $\frac{1}{2}\pi$.

From (4·5) we form estimates of the input energy spectrum E_r^i, the output energy spectrum E_r^o, and the cross-spectrum $C_r+\mathrm{i}Q_r$, namely

$$E_r^i = \langle \tfrac{1}{2} G_r G_r^* \rangle \qquad E_r^o = \langle \tfrac{1}{2} H_r H_r^* \rangle \qquad C_r + iQ_r = \langle \tfrac{1}{2} G_r H_r^* \rangle, \tag{4·6}$$

where the ensemble averages are taken for consecutive values of r, or, more accurately, by averaging quantities for the same r derived from analyses at different epochs. Since the input energy is noise-free, we may express the cross-spectrum as

$$C_r+\mathrm{i}Q_r = \langle G_r G_r^* Z_r + |N_r|\,|G_r|\,\mathrm{e}^{-\mathrm{i}\nu r} \rangle, \tag{4·7}$$

where N_r is the noise element in H_r, and ν_r its phase relative to G_r. The phase of the noise is random†, so the second term in the ensemble average is negligibly small. The admittance estimate

$$Z_r = X_r+\mathrm{i}Y_r = (C_r+\mathrm{i}Q_r)/E_r^i = \langle G_r H_r^* \rangle / \langle G_r G_r^* \rangle \tag{4·8}$$

is not biased by noise effects, whereas H_r/G_r is always greater than $|Z_r|$ by a proportion dependent on the noise : signal ratio, no matter how extensive the ensemble averaging. The sampling variability of the admittance estimate (4·8) is discussed in appendix B.

A convolution similar in form to the impulse response relation (4·2), but expressed in discrete time intervals, is

$$\hat{\zeta}(t) = \text{real part of } \sum_{s=0}^{S} c^*(t-\tau_s)\, w_s, \tag{4·9}$$

to which corresponds an admittance function

$$Z(f) = w_0 + \sum_{s=1}^{S} w_s \exp(-2\pi i f \tau_s). \tag{4·10}$$

At the discrete frequencies $f = r/355$ c/d, $Z(f)$ equals precisely Z_r in equation (4·8).

An important parameter is the coherence

$$\gamma_r^2 = \frac{C_r^2+Q_r^2}{E_r^i E_r^o}, \tag{4·11}$$

which is positively biased (to remove the bias, see appendix B). We shall use γ_r^2 in a significant way to separate the sea-level energy E_r^o into two parts, namely

$$\text{'coherent energy'} = \gamma_r^2 E_r^o = Z_r Z_r^* E_r^i, \tag{4·12}$$

which is the sea-level energy in the appropriate frequency band that may be directly ascribed to the tidal effect concerned, and

$$\text{'noncoherent energy'} = (1-\gamma_r^2) E_r^o, \tag{4·13}$$

† We include in the 'noise' such tidal components that are incoherent with the particular spherical harmonic under consideration (see § 4*c*).

which is effectively noise energy, but may contain energy coherent with other input functions.

(c) *Lag intervals and the credo of smoothness*

It is possible that an arbitrary sequence of lag intervals τ_s could be chosen along with the coefficients u_s, v_s in (9) to optimize the correspondence of (10) to a given natural system. However, there appears to be no simple rule for choosing such a sequence, apart from systematic trial and error, and after some experiments which proved tedious and unrewarding we decided to restrict the analysis to arithmetic sequences only.

With $\tau_s = s\Delta\tau$, the formalism becomes more elegant, and one may think of the convolution (9) as equivalent to fitting a Fourier series (10) to the actual admittance $Z(f)$. The Fourier series has periodicity $1/\Delta\tau$ in f, which is of course unrealistic, but quite acceptable in practice provided $1/\Delta\tau$ is greater than twice† the bandwidth ΔF within which the spectrum $G(f)$ of the spherical harmonic m, n is confined. This choice of an optimum 'lag interval' $\Delta\tau = 1/2\Delta F$ is somewhat analogous to the choice of frequency interval $\Delta f = 1/2\Delta T$ for a spectrum of a time series of duration ΔT. The effective bandwidth for the gravitational potentials P_2^1 is from 0·8 to 1·1 c/d, and for P_2^2 from 1·75 to 2·05 c/d. This suggests a bandwidth of 0·3 c/d for any of the input functions, and a corresponding 'time resolution' $\Delta\tau$ of 1·7 d approximately. Some numerical tests for Honolulu showed $\Delta\tau = 2$ days to be a good compromise, and this interval was adopted. A lag interval of 2 d seems surprisingly long; off-hand one might have expected something like 3 h, one quarter of the principal tidal period. But the essential factor is not the signal period but the interval $(\Delta F)^{-1}$ during which interference from components within the band significantly alter the signal.

The convolution is carried out for lags $\tau = 0, \Delta\tau, 2\Delta\tau, \ldots, S\Delta\tau$. It is important to decide what the maximum lag should be. The fundamental consideration is the wiggliness in the admittance function $Z(f)$. If the shortest wiggles have a 'wavelength' of F c/d, then $S\Delta\tau = 1/F$ is the appropriate choice for the maximum lag. Again this is more familiar in the time domain: if T is the shortest period present, then the spectrum extends to some maximum frequency $1/T$. We find no evidence for wiggles in $Z(f)$ shorter than $\frac{1}{6}$ c/d, and accordingly have terminated the convolution at a lag of 6 d ($S = 3$). In reverse, if wiggles shorter than $\frac{1}{6}$ c/d should occur, these will be smoothed out by the termination in lag times. In this way we impose a 'credo of smoothness' on oceanic response characteristics. We do not believe, nor will we tolerate, the existence of very sharp resonance peaks. Our results so far confirm a degree of smoothness consistent with the adopted limit.

According to the Nyquist (or sampling) theorem, a curve needs to be sampled at half the shortest wavelength in order to be adequately represented by the discrete values. With respect to the oceanic admittance, this implies sampling at $1/(2F) = \frac{1}{12}$ c/d $\approx 0{\cdot}08$ c/d. In fact, the spectrum $G(f)$, and therefore information about $Z(f)$, is concentrated in narrow groups separated by $\Delta f = 1$ c/m $\approx 0{\cdot}03$ c/d, and this sampling is at closer intervals than the limit 0·08 c/d imposed by the credo of smoothness.

We have here two entirely independent considerations concerning frequency resolution. The ocean's capacity for sharp resonances imposes certain requirements on Δf if the response is to be adequately sampled; the inclination and ellipticity of the Moon's orbit determine

† $1/\Delta\tau = 1 \times \Delta F$ is theoretically possible, but would entail a discontinuity near the limits of the frequency band, making for slow convergence of the series.

the best available sampling. Is it adequate? The fact is that the Moon 'oversamples' the response by a factor of 2 or 3. Higher order splitting is associated with even more severe oversampling. The advantage of the response method over the harmonic method is closely related to the degree of oversampling.

The relative advantage of the response method over the harmonic method increases then with the complexity of the spectral input and diminishes with the complexity of the admittance. In the limiting case of a continuum input (infinite oversampling), the response method is the only possible method; for unresolved lines it is the only practical one.† But the advantages may be there even for a resolved line spectrum. At the same time the imposed smoothness of admittance does impose upon the user the responsibility of having generated realistic input functions, and in this sense the response method requires more care than the harmonic method.

(*d*) *Realizability of response*

Equation (10) restricts the admittance $Z(f) = X(f) + iY(f)$ to orthogonality in X and Y. This restriction has been dropped by permitting negative as well as positive values of s. For then

$$\zeta(t) = \sum_{s=-S}^{S} [u_s\, a(t - s\Delta\tau) + v_s\, b(t - s\Delta\tau)], \tag{4·14}$$

$$\left.\begin{aligned} X(f) &= u_0 + \sum_{s=1}^{S} [(u_s + u_{-s}) \cos(2\pi f s\Delta\tau) + (v_s - v_{-s}) \sin(2\pi f s\Delta\tau)], \\ Y(f) &= v_0 + \sum_{s=1}^{S} [(u_s - u_{-s}) \sin(2\pi f s\Delta\tau) - (v_s + v_{-s}) \cos(2\pi f s\Delta\tau)]. \end{aligned}\right\} \tag{4·15}$$

This permits $2S+1$ degrees of freedom as compared to $S+1$, without exceeding the limits discussed in the preceding section.

The procedure apparently violates causality, the prediction (14) depending on both future and past values of the input functions. An equivalent statement is that the admittance (15) is not physically realizable. But since our knowledge is limited to a few narrow frequency bands, we are under no obligation to fit $Z(f)$ over all frequencies. In fact, the periodic representation of $Z(f)$ inevitably makes (15) invalid outside the known bands. (Restriction to positive lags would lead to an admittance (15) which is realizable, but still not applicable outside the bands because of the imposed periodicity.)

(*e*) *Multiplets and multiple components*

We now turn to certain fundamental properties of the input functions. The difficulty of the subject is associated with the complexity of the input spectra as well as the multiplicity of processes associated with each of the spectral lines.

What appears as single lines at 0, 1, 2, ... c/d in the analyses of 1 day's record is split into multiplets separated by 1 c/m in the analyses of 1 month's record. In turn, each of these lines becomes a multiplet with c/y separation when a year's record is analysed, and once again these lines are split at nodal frequencies when 18·6 y are analysed.

Each of the spectral lines contains some contribution (possibly quite small) from Moon *and* Sun. The solar angles $h_\odot$, $p_\odot$ appear in the lunar parameters because of the strong

† The f, u factors (§ 2(*b*)) are a case in point.

perturbation of the Moon's motion by the Sun; the lunar angles appear in the solar parameters because of the perturbation of the Earth's motion by the Moon.

Nonlinearities in the Keplerian laws and Newtonian mechanics produce sum and difference frequencies that are responsible for the complexity in the 'linear' input functions. Hydrodynamic nonlinearities inherent in the Navier–Stokes equation lead to additional splitting and produce overlapping frequencies. The peculiarity of the situation arises then from the circumstance that the Kepler–Newton nonlinearities are in series with the Navier–Stokes nonlinearities.

The **k.f** space introduced in § 2·2 contains all possible frequencies, allowing for celestial and terrestrial nonlinearities. In reverse, every point in **k.f** space is affected by the Sun and Moon and by hydrodynamic nonlinearities. Strictly speaking, there are no pure lines. But it is convenient to speak of mixed lines† in the sense that they contain *significant* multiple components. For example, (i) mixed luni-solar gravitational tides, principally K_1 and K_2 (but there is no point ever in separating lunar from solar gravitational effects); (ii) mixed linear and shallow-water tides; and (iii) mixed gravitational and radiational lines that occur in narrow bands, about 4 c/y wide, of groups (0 0) (1 1), and (2 2).‡

The credo of smoothness permits the separation of multiple components.

(*f*) *Sequential and lumped analyses*

In the following discussion of tidal observations we have used two distinct (but closely related) methods of estimating admittance. In the *sequential* scheme we first perform the cross-spectral analysis between the observed sea level $\zeta(t)$ and the input function $c_2^m(t)$ to obtain the ensemble-averaged admittances $(Z_r)_2^m$ (equation (4·8)). Smoothed curves are fitted to the point estimates of $(Z_r)_2^m$ by least squares, with weights inversely proportional to the sample variances. The second degree harmonics of the gravity potential multiplied by these smoothed admittances is then subtracted vectorially from the sea-level spectra to form residual spectra. These residuals are then compared with $c_3^m(t)$ in exactly the same fashion and new residuals formed. These in turn are compared to radiational inputs, etc.

Multiple components were separated as follows: the spectral estimates H_r of sea level ζ for any double component may be written

$$H_r = Z^*(f)\, G_r + Z'^*(f)\, G'_r + N_r, \tag{4·16}$$

where G_r and G'_r are the respective input spectra, and Z^* and Z'^* are the conjugates of the associated admittances. ($Z'^*G'_r$ cannot be classed with the noise N_r, as in (7), because its phase relative to G_r is constant). We cannot solve (4·16) for both Z and Z', even when the noise is reduced by ensemble averaging. The six equations for the cross-spectral elements G^*H, G'^*H, G^*G' are interdependent, and reducible to two independent equations for the four unknown X, Y, X', Y'. We therefore need a least-squares solution for two or more consecutive values of r for which the admittances Z and Z' can be regarded as constant, or slowly varying. Strictly even the least-squares solution is possible only if the ratios G_r/G'_r vary with r, but in practice this seems to be the case. The equations involved are straightforward.

† We shall not consider nonidentical frequencies which merely differ by a very small quantity, such as $(f_4 - 2f_5)$, since in all such cases listed by Doodson at least one of the amplitudes involved is negligibly small.

‡ Group (0 0) contains the radiational inputs α_1^0, α_2^0. Group (1 1) has a triplet input χ_1^1, χ_2^1, c_2^1. Group (2 2) contains χ_2^2, c_2^2.

An alternate scheme (which we adopted) is to perform a *lumped* analysis involving all selected input functions in one operation (§ 4 (*g*)). This yields the weight matrix from which the admittances are computed by the appropriate Fourier transforms (equation (4·15)). The coherence at different parts of the spectrum is automatically taken into account. Multiple inputs are separated subject to the credo of smoothness.

The sequential scheme has certain pedagogical advantages, but the lumped analysis is more straightforward and precise and does not impose conditions concerning the relative magnitudes of successive input functions.

(*g*) *The weight matrix and prediction variance*

It remains to comment on the computations involved in deriving the weights u_s, v_s for a particular sea-level record. The predicted sea level is given by

$$\hat{\zeta}(t) = \sum_{m,n} \sum_{s} [(u_n^m)_s a_n^m(t-s\Delta\tau) + (v_n^m)_s b_n^m(t-s\Delta\tau)] + \text{radiational terms} + \ldots, \quad (4\cdot17)$$

with the weights determined by the condition that the time average

$$\sigma^2 = \langle [\zeta(t) - \hat{\zeta}(t)]^2 \rangle$$

be a minimum. We can use the general notation

$$\hat{\zeta}(t) = \sum_i w_i c_i,$$

with the understanding that w_i designates any of the weights $(u_n^m)_s$ or $(v_n^m)_s$, and c_i the associated lagged input $a_n^m(t-s\Delta\tau)$ or $b_n^m(t-s\Delta\tau)$, whatever the value of m, n, s, and whatever the source of the terms, gravitational, radiational, or otherwise. The weights w_i are found by solving the matrix of linear equations

$$[M_{ij}]\,[w_i] = [R_i], \quad (4\cdot18)$$

where

$$M_{ij} = \langle c_i c_j \rangle, \quad R_i = \langle c_i \zeta \rangle. \quad (4\cdot19)$$

Mean values are removed from $\zeta(t)$ and $c_i(t)$ when necessary.

For long records the mean covariances between different tidal species are very small and the matrices may be split into separate blocks,† one for the spherical harmonics contributing to each species m, and inverted separately. The minimum value of σ^2 is then

$$\sigma^2_{\text{min.}} = \langle \zeta^2(t) \rangle - \sigma_0^2 - \sigma_1^2 - \sigma_2^2 - \ldots.$$

We refer to

$$\sigma_m^2 = \sum_i w_i^{(m)} R_i^{(m)}, \quad (4\cdot20)$$

as the 'prediction variance' for species m, with the meaning that the convolution prediction reduces the variance of residual (observed minus predicted) sea level by σ_m^2. It is not in general the same as the variance of the prediction itself, which is

$$\langle [w_i^{(m)} c_i^{(m)}]^2 \rangle.$$

As in spectral analysis, 355 days is a good period for summing the cross-products, and 19×355 days is considerably better. In order to compare prediction variances for different

† This is not only a matter of mathematical convenience; in fact, accuracy of the prediction depends on the precision to which the matrix is separable, because of the band-limited validity of our admittances.

combinations of variables, it was found important to compute the mean products of lagged quantities with high precision. For example, if $c_i = a_2^1(t)$, $c_j = a_2^1(t-\Delta\tau)$, $c_k = a_2^1(t-2\Delta\tau)$, and 3 h values are summed for 355 days, then

$$M_{ij} = (2840)^{-1} \sum_{t=0}^{2837} c_i c_j, \quad \text{not} \quad (2840-\Delta\tau)^{-1} \sum_{t=\Delta\tau}^{2837} c_i c_j,$$

and M_{jk} may not be assumed equal to M_{ij} as in conventional time series analysis. In a comparison of prediction variances arrived at by slightly different schemes it was found desirable to form the summed products (19) by integer arithmetic. (The computers used, CDC 1604 and 3600, permit storage of integers up to 15 significant figures.)

5. Results for Honolulu

(*a*) *The observations*

We chose Honolulu for our first analysis. It is an oceanic island relatively free from shallow water effects. About fifty years of hourly readings were available and these have been carefully edited and stored on magnetic tape.† Tides of diurnal and semidiurnal species are of about equal intensity. We analysed most thoroughly the 20×355 day period 25 July 1938 to 1 January 1958; in the very low-frequency range we used all available 52 years, 1905 to 1958. Two short gaps, 11 days in 1950 and 13 days in 1953, and a larger gap of 50 days in 1942, were filled by conventional harmonic prediction with linear trends. The hourly series were smoothed by a low-pass filter with cut-off at 4 c/d, and thinned 3:1 to give 8 readings per day. This reduced the bulk of the subsequent computations. The resulting 'Nyquist' frequency of 4 c/d is quite high enough, because tidal energy at frequencies above 3 c/d is negligible.

(*b*) *The spectrum at c/m resolution*

The heights of the columns in the upper two panels of figure 1 refer to the spectra, E_r^i and E_r^o, of equilibrium‡ ($n=2$) and recorded sea level. The two time series were subjected to identical filtering processes, and to ensemble averaging over 19 consecutive periods of 355 days (§ 4 (*b*)), leading to estimates of the constituents $(k_1\ k_2\ k_3)$ at 1 c/y resolution. The plotted group estimates $(k_1\ k_2)$ at 1 c/m resolution were obtained by forming the averages

$$(k_1\ k_2) = \sum_{k_3=-3}^{k_3=3} (k_1\ k_2\ k_3)$$

over seven adjoining constituents.

† The methods are described in 'A user's guide to BOMM; a system of programs for the analysis of time series', by Bullard, Oglebay, Munk & Miller, Institute of Geophysics and Planetary Physics, University of California, La Jolla, April 1964 (unpublished).

‡ In § 5 we use equilibrium level

$$a_n^m(t)\ U_n^m(\theta, \lambda), \quad \theta = 68^\circ\ 42', \quad \lambda = 202^\circ\ 13',$$

rather than the gravitational potential $a_n^m(t)$ for the input function in equation (4·5). For a fixed m, n the two functions differ only by a constant amplitude factor and phase shift. The physical meaning of equilibrium level is somewhat clearer and there is some advantage in referring to it, provided the station does not lie close to a nodal colatitude of one of the spherical harmonics. The discussion of prediction variance (§ 6) is based on inputs $a_n^m(t)$, $b_n^m(t)$.

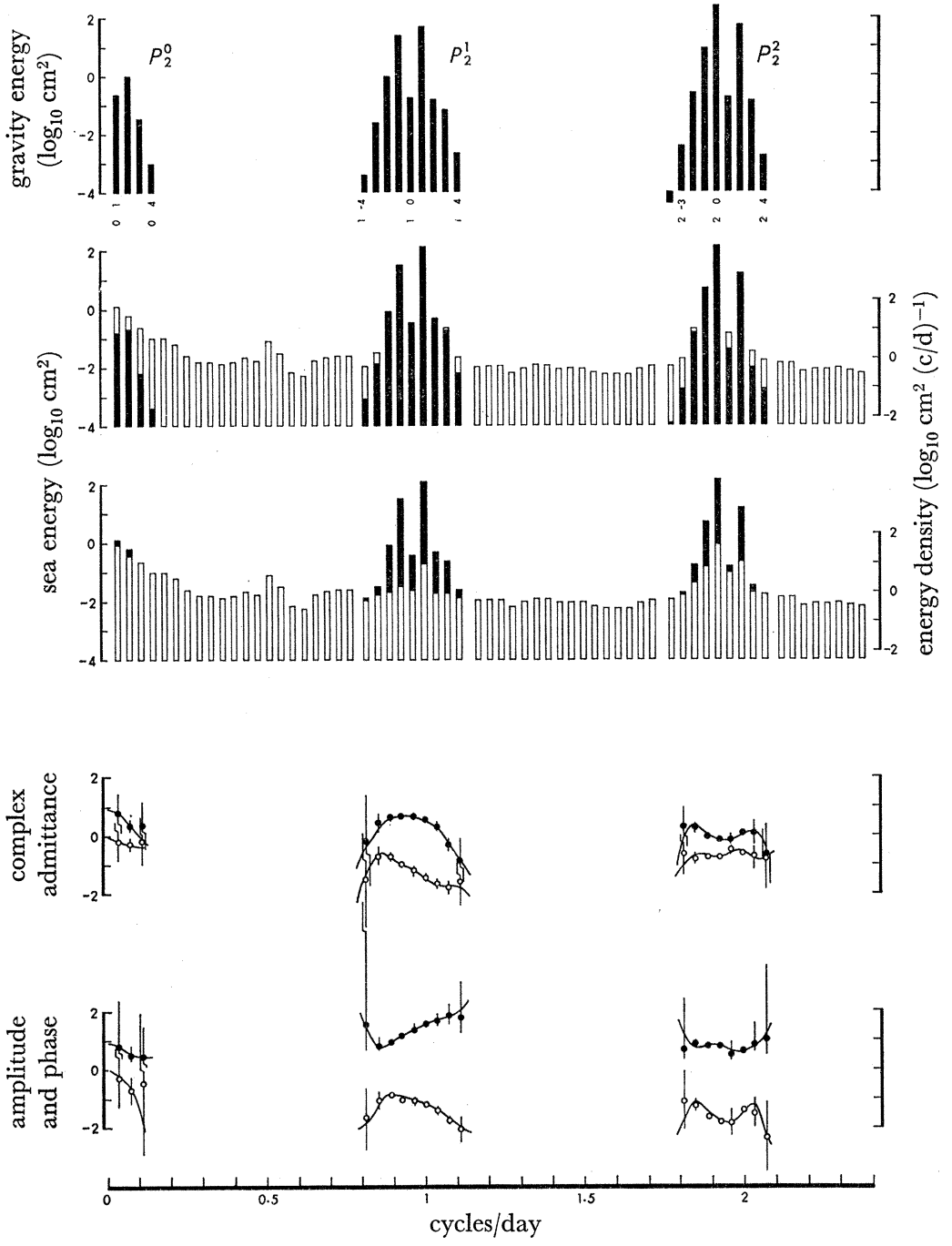

FIGURE 1. Honolulu tide spectra at 1 c/m resolution for spherical harmonics of degree 2. P_2^0, P_2^1, P_2^2, refer to tidal species 0, 1, 2 respectively. The upper panel shows the energy of the gravitational equilibrium tide at Honolulu relative to 10^{-4} cm^2; some 'Doodson group numbers' are written below the columns. In the next two panels, the observed sea spectrum is designated by the total height of the columns. In the upper of the two, the height of the *filled* portion designates the energy *coherent* with the equilibrium tide; in the lower, the height of the *unfilled* portion designates the *noncoherent* energy. The left scale refers to energy per column, the right scale to energy per c/d. In panel 4, the filled circles refer to the real part, the open circles to the imaginary part of the admittance. In panel 5, they refer to |admittance| and phase lead in radians, respectively. The vertical lines show the 95 % confidence limits of the circles. The curves represent the admittance functions derived from the convolution process.

In the *equilibrium* spectra the significant energy ($\sim 10^{-4}$ cm^2 or more) is contained in the groups (0 1) to (0 4), (1 −4) to (1 +4) and (2 −4) to (2 +4) with energy gaps between these groups. In the *recorded* spectra the same groups are prominent, but there are no gaps between. Rather, a plateau of roughly 10^{-2} cm^2 per group is attained, corresponding to an energy density of 1 cm^2/c/d. Presumably this is the nontidal continuum which underlies the tidal line spectrum (Munk & Bullard 1963).

The hypothesis can be tested by considering separately the *coherent* and *noncoherent* parts of the recorded energy,

$$\gamma_r^2 E_r^o \quad \text{and} \quad (1-\gamma_r^2) E_r^o,$$

corresponding to the filled and unfilled portions of the columns. Panels 2 and 3 contain the same information, the two displays being necessitated by the logarithmic scale. In columns containing largely coherent energy the noncoherent portion is perceptible only in panel 3, and vice versa. It will be seen that the coherent recorded energy corresponds closely to equilibrium energy. Noncoherent energy fills the frequency space between prominent groups; furthermore, it can be traced *across* the groups, and there it is found to peak, particularly with respect to the group (2 0) which contains the strong M_2 constituent. This is the 'tidal cusp', discussed by Munk, Zetler & Groves (1965). (However, as we shall see later, their simple explanation in terms of interaction with the low frequency continuum does not fit the facts.) The relatively large fraction of noncoherent energy in the solar groups (1 1) and (2 2) will be ascribed to radiational processes.

The noncoherent energy contributes a very small fraction to the total energy in species 1 and 2. The reverse situation applies for species 0. The anomalous peak and trough in the continuum at about 0·5 c/d has been attributed by Longuet-Higgins (1965) to a resonance effect in the theory of planetary waves.

The circles in the lowest two panels of figure 1 show the admittance X_r, Y_r and $|Z_r|$, arg (Z_r), derived from (4·8). The confidence limits (appendix B) illustrate the unreliability of tidal estimates whenever the energy is below continuum level. The admittances are obviously far from constant within any tidal species, as already known from published tables of phase lag κ (essentially the same as $-\arg(Z)$); but the variation in admittance is sufficiently smooth to be simulated by the convolution process discussed earlier. In fact, the plotted curves represent the admittances from a lumped analysis subject to the credo of smoothness; input parameters are given in table 2, § 6.

The admittance circles for the luni-solar groups (1 1) and (2 2) were derived by a special treatment. Since the strongest lines in the groups contain multiple input functions from nonseparable gravitational and radiational potentials, the admittance estimators used for the lunar groups are not applicable. However, there are some nontrivial purely lunar lines in these solar groups which modulate the lunar parts of K_1 and K_2 at the nodal cycle of 18·6 years, the most important being (1 1 0 0 1) and (2 2 0 0 1). The energy at these lines is certainly not affected by radiation. We isolated these, and some lesser neighbouring lines by analysing the modulations of the K_1 and K_2 constituents over 19 successive years, deriving admittances from their cross-spectral components as before. The resultant admittances, as plotted at the appropriate frequencies, left a very low residue of 'noise'. They fit well into the general trend suggested by the neighbouring lunar zones.

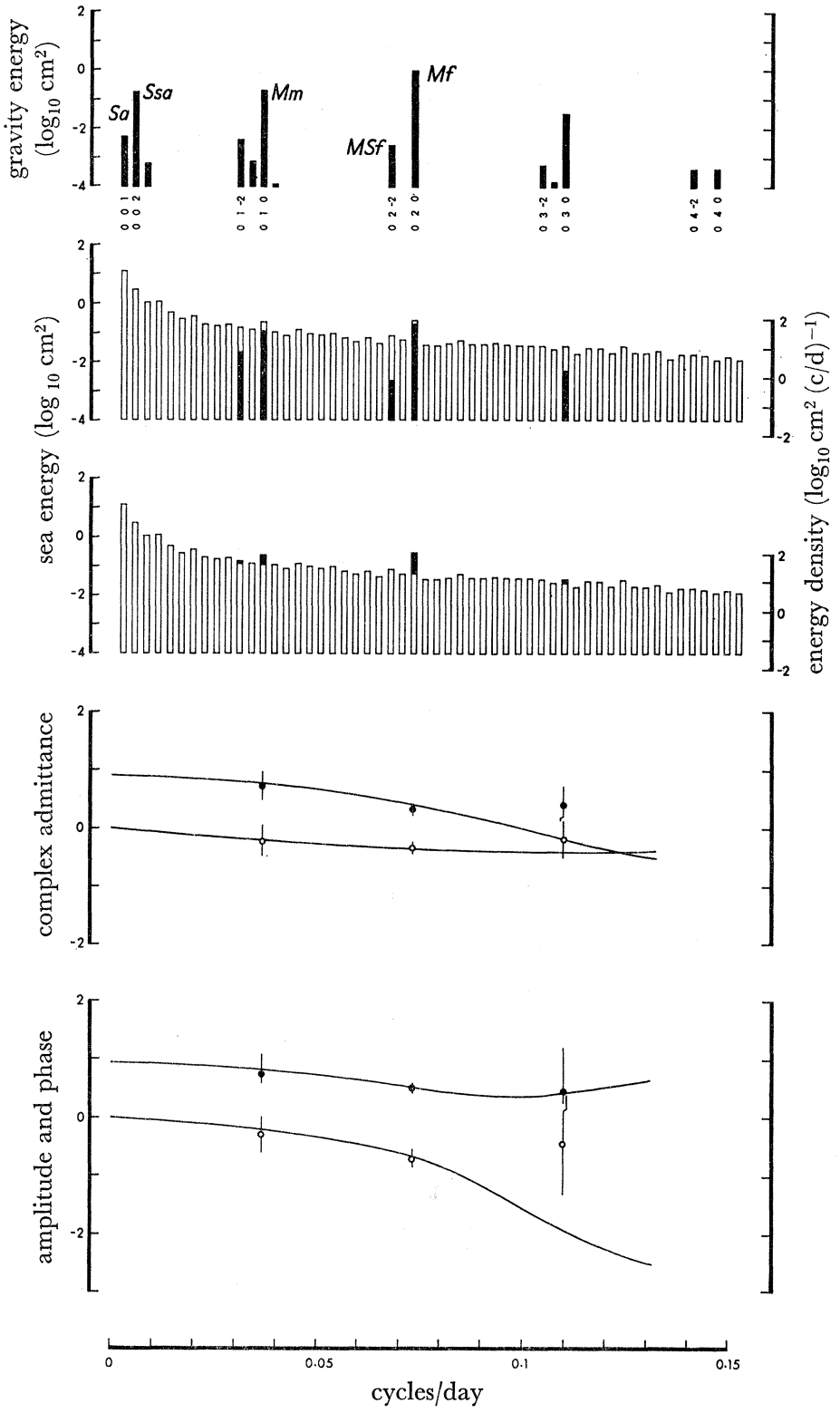

FIGURE 2. Honolulu tide spectra at 1 c/y resolution for the low-frequency spherical harmonic P_2^0. Some 'Darwin' symbols and 'Doodson' constituent numbers are included in the upper panel. Legend is otherwise as in figure 1.

(*c*) *The spectrum at c/y resolution*

Figures 2 to 4 show the same spectra and admittances at greater resolution. Here we see the tidal 'constituents' named by Darwin and other constituents of lesser importance, usually unnamed or allocated to nonlinear 'over-tides'. In figure 2, the constituent labelled *MSf* is the linear lunar input at (0 2 −2), not the S_2-M_2 nonlinear interaction at the same frequency. The coherent energies at 1 and 2 c/y (*Sa* and *Ssa*) were not plotted because they

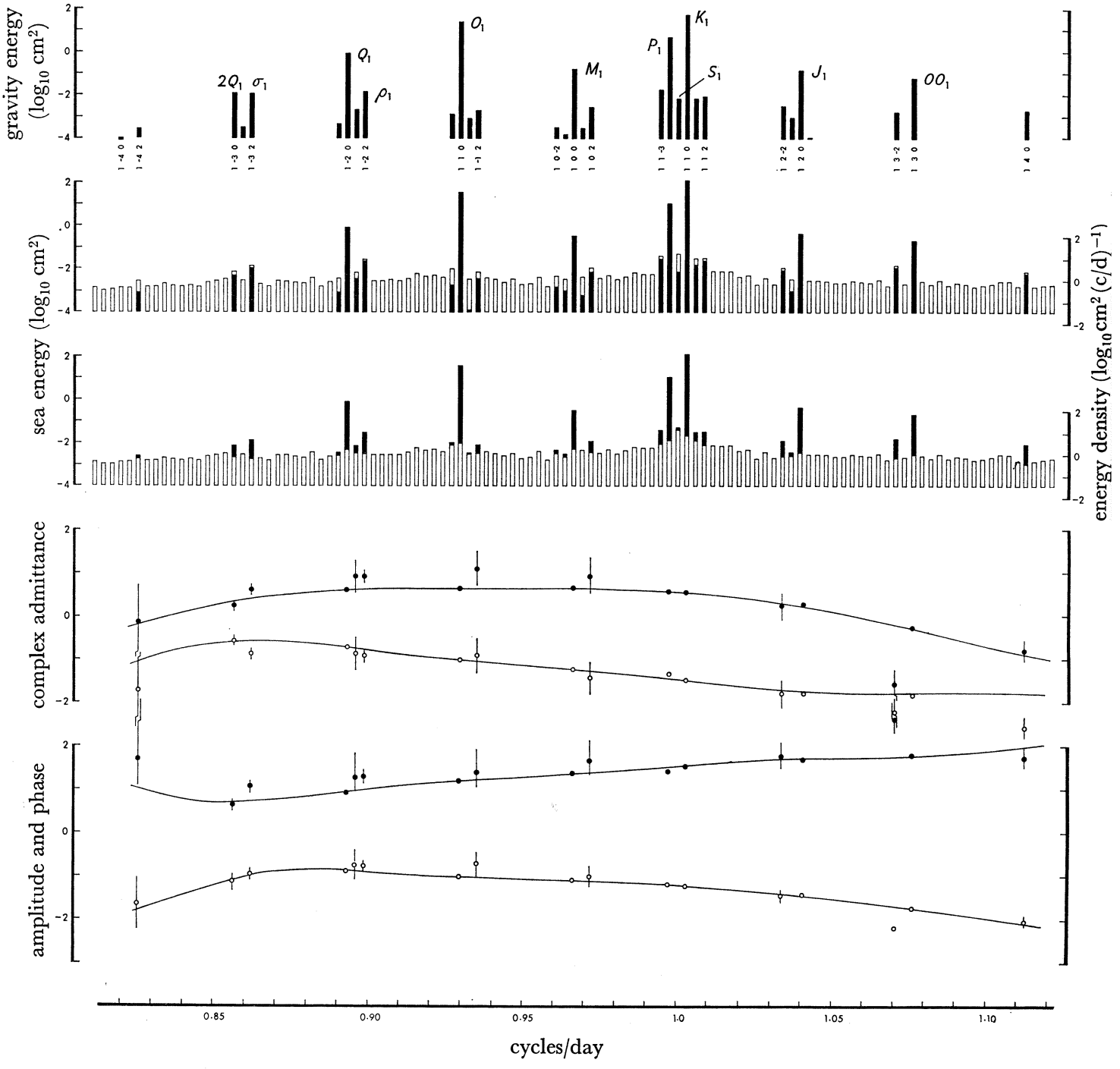

FIGURE 3. Honolulu tide spectra at 1 c/y resolution for the diurnal spherical harmonic P_2^1.

include radiational energy and give anomolous admittances. Separation of gravitational and radiational energy is possible by the method of multiple components. A better procedure is the lumped analysis on which the plotted curves are based. These curves approach a gravitational admittance of $Z = 0{\cdot}92$ at zero frequency. The reliability of this limit is about the same as that of the estimate at 1 c/m, namely $\pm 0{\cdot}24$ at the 95 %

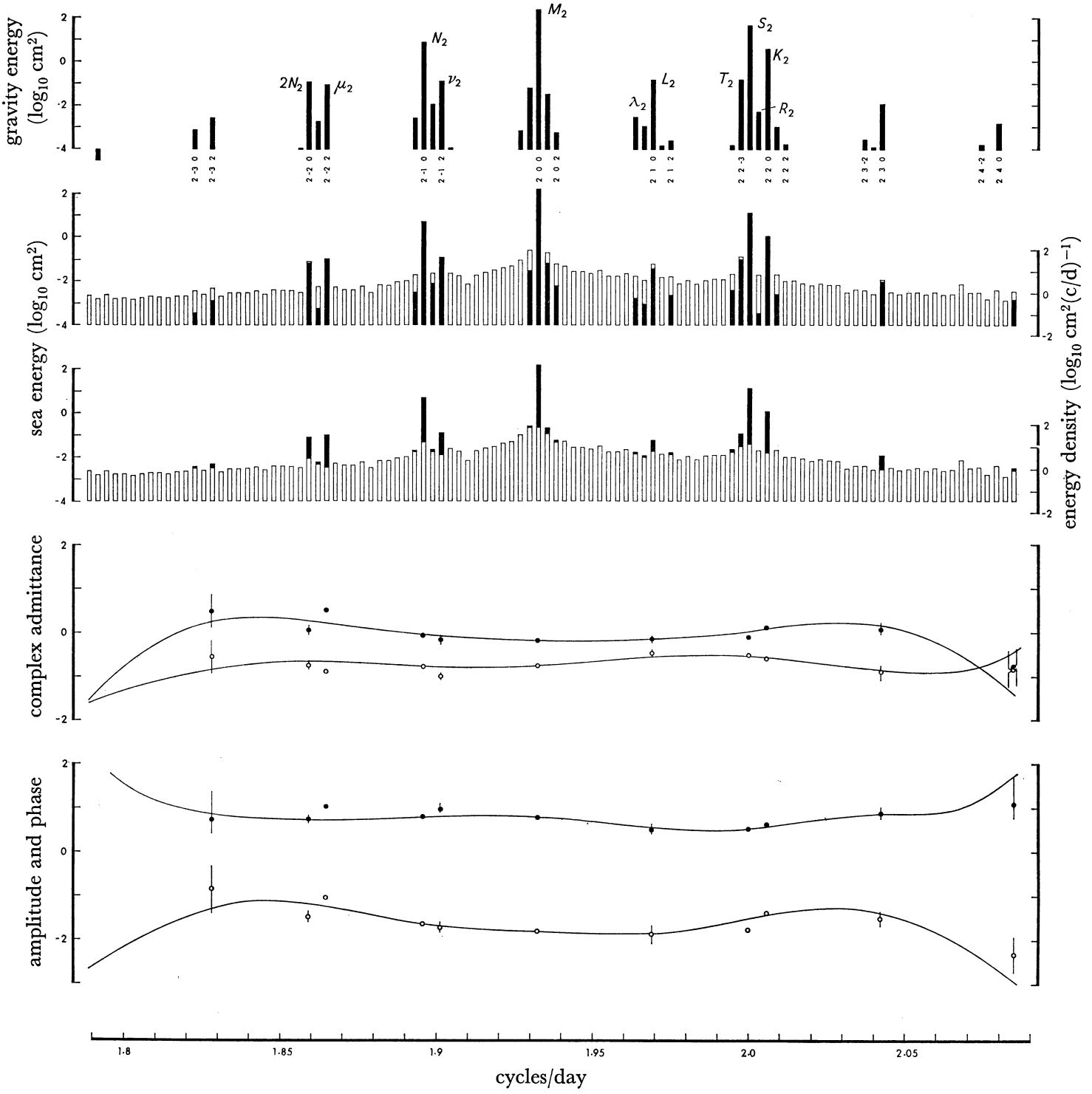

FIGURE 4. Honolulu tide spectra at 1 c/y resolution for the semidiurnal spherical harmonic P_2^2.

confidence level. The corresponding static limit in terms of the customary Love number notation is

$$1+k-h = 1+0{\cdot}29-0{\cdot}59 = 0{\cdot}70.$$

Cusps in the continuum are more prominent at the present resolution, particularly those centred on M_2, S_2 and K_1.† Significant departures from the smoothed admittance (as produced by the lumped analysis) can be associated with pairs of constituents separated by 2 c/y (declinational splitting); for example, between (2 −2 0) and (2 −2 +2), and

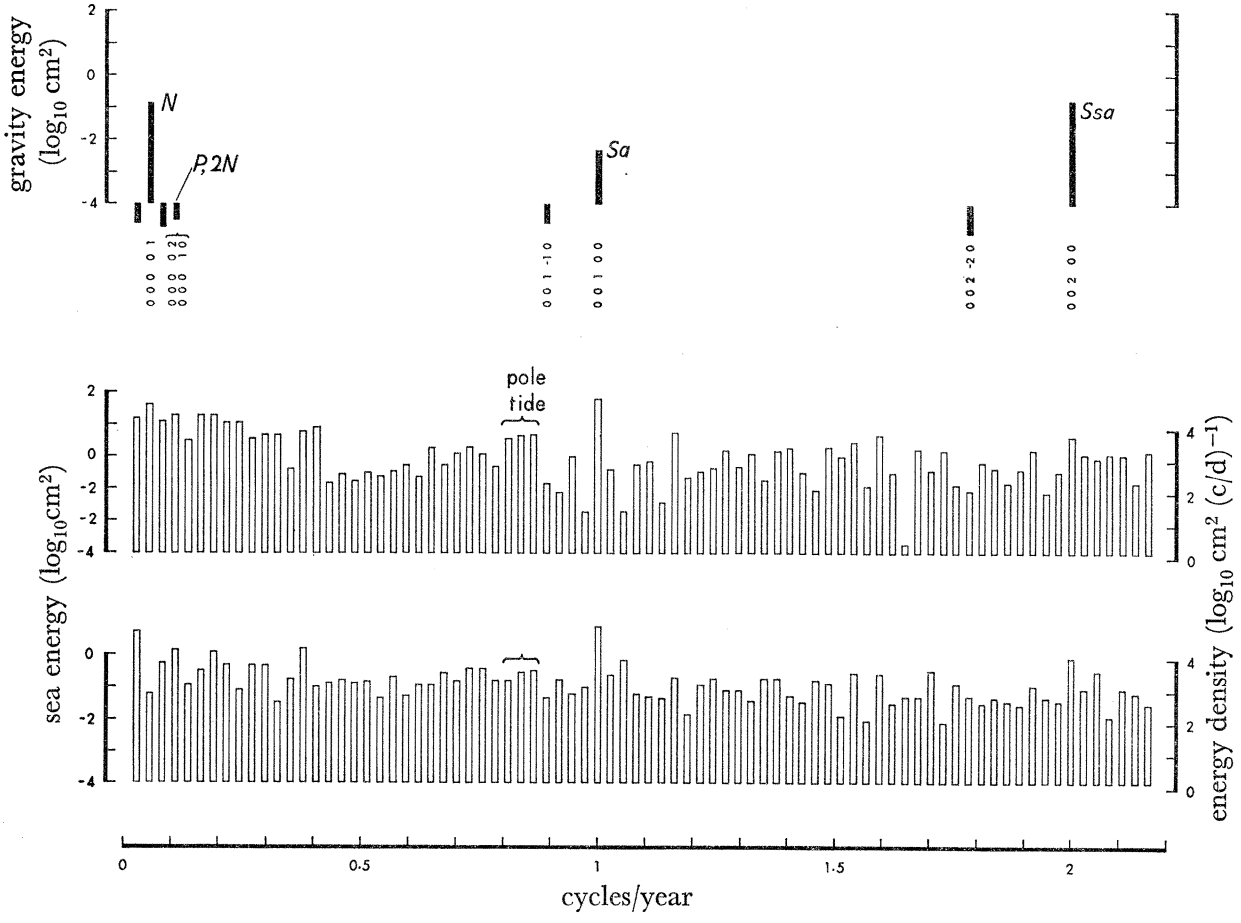

FIGURE 5. Honolulu tide spectra at 1/37 c/y resolution for the lowest frequencies in spherical harmonic P_2^0. The 'Doodson' numbers in the upper panel refer to (k_1 k_2 k_3 k_4 k_5) in equation (2·3). The lower panels show sea energy for the periods 1905·14 to 1942·14 and 1920·86 to 1957·86 respectively. A plot of mean sea level covering both periods is shown in figure 6.

between (2 −1 0) and (2 −1 +2). Presumably this 'jitter' in the admittance is due to triple interactions caused by friction. The effects of cusp and jitter on the overall results of the present study are slight, but they are worthy of further consideration (§ 9).

The admittance points for the K_1 constituent are those derived from the nodal modulations. The small anomaly in the admittance for P_1 is an indication of radiation effects; the anomaly could be removed by the method of multiple inputs. Other indications of radiation are the prominent noncoherent residuals of S_1 and S_2. It is interesting to note that the phase

† The weak K_1 cusp appears to be centred on S_1 because the radiational contributions have not been eliminated at this stage.

lead at S_2 is slightly larger than that at M_2, making Honolulu one of the relatively rare places (even among oceanic islands) where the 'age of the tide' is not positive.

(*d*) *The spectrum at nodal resolution*

Figure 5 was derived from two overlapping 37 y records, and represents the highest spectral resolution we attempted.† We show only the results for species 0. Each column has one degree of freedom, as opposed at 19 in figures 2 to 4, and 247 in figure 1. The noise level at the low frequencies is too great for any of the tidal lines to stand out except the (mainly radiational) annual and semi-annual constituents. Three adjoining lines centred at 0·85 c/y are probably associated with the 14 month 'pole-tide' due to the wobble of the Earth

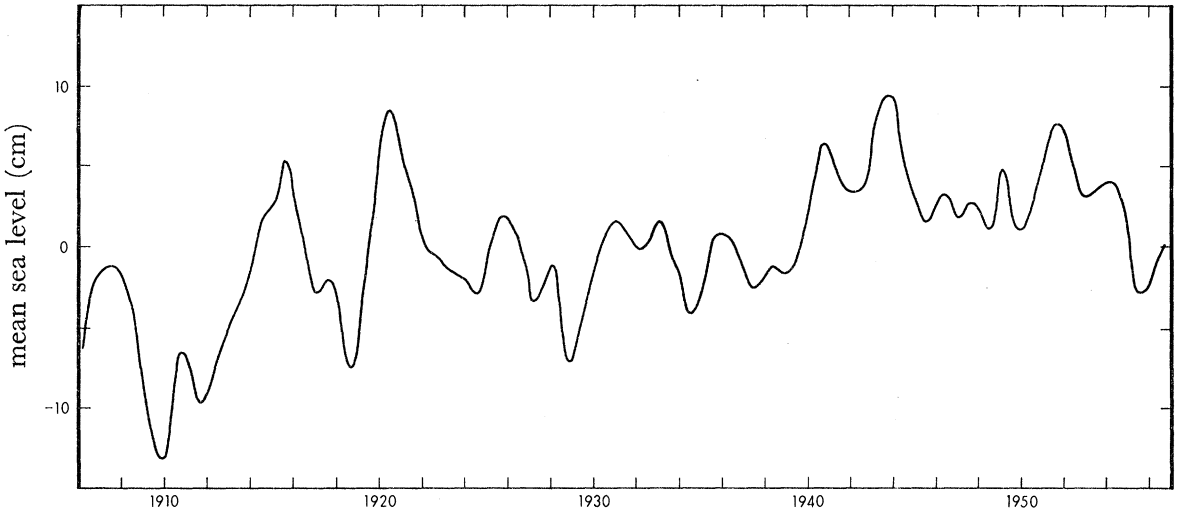

FIGURE 6. Honolulu 'mean' sea level, with frequencies above 2 c/y attenuated.

(Haubrich & Munk 1959), but their energy can scarcely be said to rise convincingly above the continuum. Even the prominent 18·6 y 'nodal tide', N, is indistinguishable. The dominance of the low-frequency noise is also clear from the smoothed sea-level record plotted in figure 6. Variations with a time scale of decades are principally due to winds and pressure, to changes in sea temperature, to global changes in sea level associated with the melting of glaciers and ice caps, and to the up-and-down movement of continental blocks.

(*e*) *The spectrum for gravitational harmonics of degree* 3

The stronger lines in $a_3^m(t)$ are separated from those in $a_2^m(t)$ by multiples of the perigee frequency f_4 and nodal frequency f_5 (see Doodson's 1921 schedules). In an analysis for tides of degree 2 over 19×355 days $= 2{\cdot}087$ perigee cycles $= 0{\cdot}992$ nodal cycles, the relative phase ν_r of third degree tides pass uniformly through nearly integral multiples of 2π. Consequently, the energies of P_2^m and P_3^m are separable; in the analysis for P_2^m, the P_3^m tides appear as noncoherent energy.

Spectra and admittance points in figure 7 have been obtained by sequential analysis, admittance curves by lumped analysis. The energy of P_3^m is generally four orders of

† As a matter of minor interest, the line at (0 0 1 −1 0) is not included in Doodson's 1921 schedules, though above his threshold level. This is the only such case we have found.

magnitude below that of P_2^m, but there are significant third-degree contributions to groups (1 0) and (2 $\pm$1), and predominant contributions to the ter-diurnal species. Apart from the low-frequency harmonics there was sufficient coherent energy to yield plausible

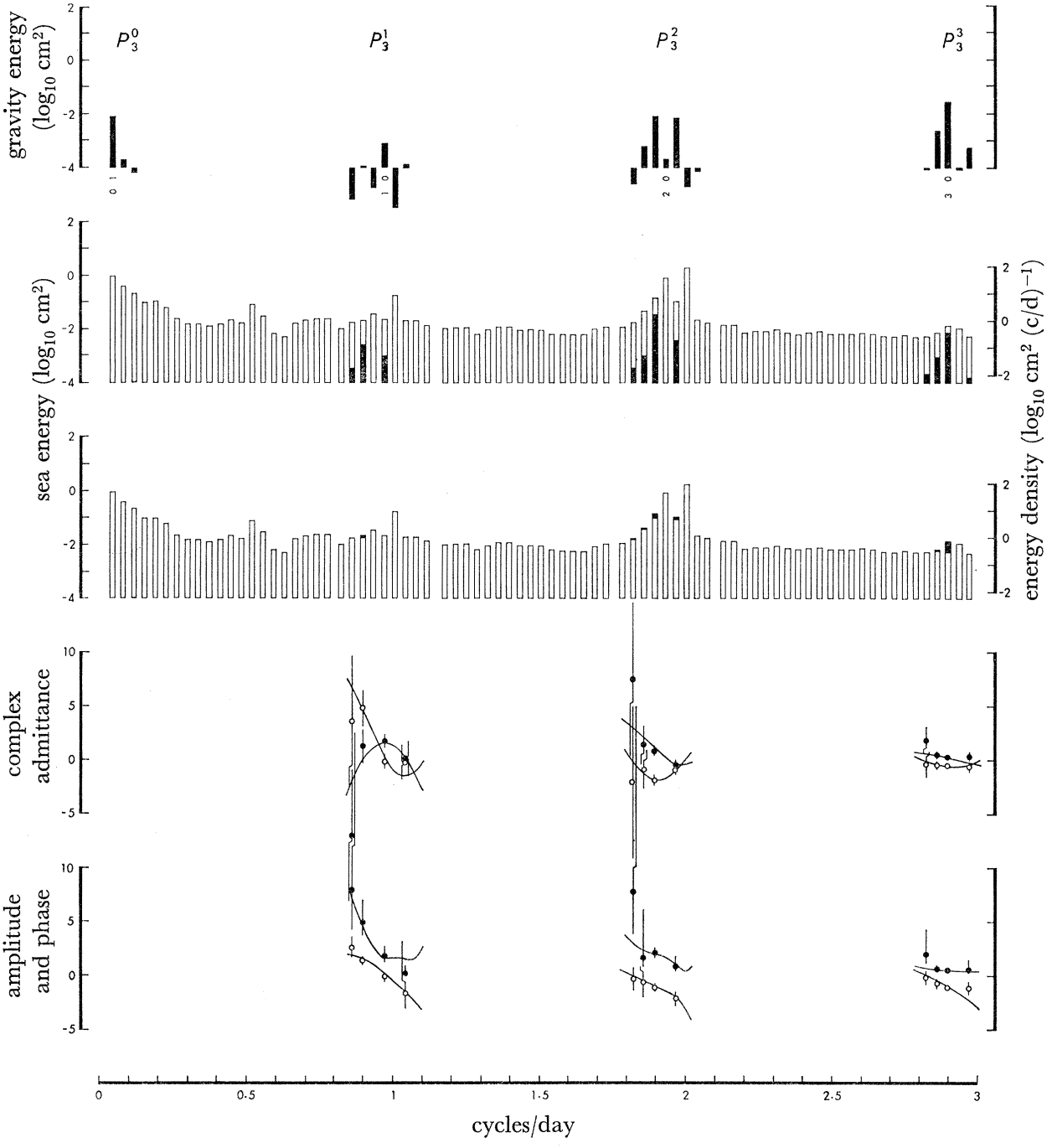

FIGURE 7. Honolulu tide spectra at 1 c/m resolution for spherical harmonics of degree 3. The display is analogous to that in figure 1, except that degree 2 tides have been removed from the sea energy.

estimates of admittance. It is interesting to note that these admittances are quite different in magnitude and general shape from the second-degree admittances. Therefore, there is no justification in the customary procedure to allow for third-degree harmonics by combining

them with second-degree harmonics in the same proportion and phase as they occur in the equilibrium tide.

One is tempted to ascribe the relatively large noncoherent energy in group (3 1) to shallow-water interaction between diurnal and semidiurnal tides. But such an effect must be dominated by the MK_3 line (due to interaction between K_1 and M_2); yet the sea-level

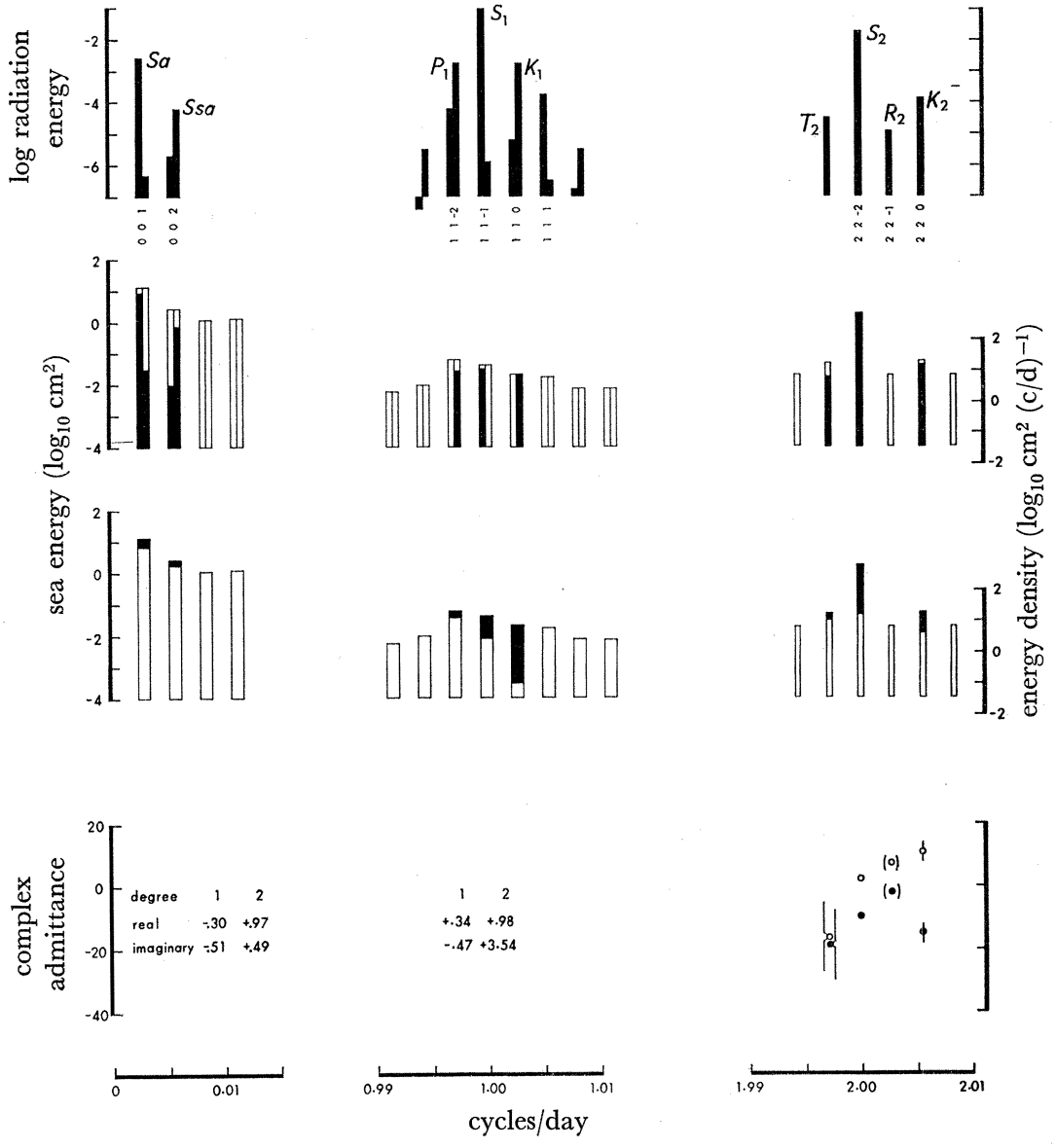

FIGURE 8. Honolulu radiational tide spectra at c/y resolution for spherical harmonics of degrees 1 (left portion of split columns) and degree 2 (right portions). The upper panel shows the energy of the radiational potential at Honolulu relative to 10^{-7} unit. For species 0 and 1 numerical values of the admittance (assumed constant) are entered. Circles in parentheses for species 2 have confidence limits too wide to be reliably computed.

spectra at c/y resolution (not reproduced here) show the energy of MK_3 to be about the same as its neighbours. At any rate, a quite trivial amount of energy is involved. Sea-level energy hardly rises in the 4 c/d zone. All these results confirm that bilinear interaction at Honolulu is unimportant.

(*f*) *Radiational tides*

Upon subtraction of all gravitational inputs of degrees 2 and 3 we are left with residuals that can be examined for radiational effects. For input functions we use $\alpha_n^m(t)\ U_n^m(\theta, \lambda)$ where $\alpha_n^m(t)$ is the fractional variation in radiation (appendix A). The results of such an analysis in the solar groups (0 0), (1 1) and (2 2) is shown in figure 8. The radiational analysis is complicated by the existence of harmonics of degree 1 (these are absent from the gravitational potential). It is seen from the top panel that the radiational inputs of degree 1 are relatively strong for *Sa* and S_1; in comparison, the gravitational input into *Sa* and S_1 is relatively weak. Radiational spectra of degree 2 resemble the solar gravitational spectra.

Radiational harmonics of degrees 1 and 2 contain precisely the same frequencies (of the form k_1 c/d$+k_3$ c/y). The two admittances have been separated by the method of multiple components assuming constant admittances within groups (0 0) and (1 1). Values are given in the bottom panel. Radiational effects are seen to account for significant amounts of energy at 1 and 2 c/y. Results in the diurnal range are confused, possibly because of inaccuracies in the subtraction of the gravitational effects, but the coherent energy is considerable, particularly at 1 c/d where the gravitational input is trivial.

Individual admittances were computed for a radiational input P_2^2. There is no input of degree 1, and the only other possible input is a radiational P_4^2, which appears to be negligible (though not so insignificant as the gravitational P_4^2). Admittances for four constituents are plotted, but some may be unreliable, and a constant admittance derived for S_2 would probably be a fair representation.

The radiational sea-level energy at 2 c/d may be represented as a wave of 1·8 cm amplitude with maximum occurring 6 h 25 min after the Sun's transit (i.e. a phase lead of 2·93 rad). The S_2 atmospheric pressure tide in the tropics has a maximum close to 10 h, and a minimum 4 h after transit. Therefore, the radiational ocean tide at Honolulu lags the inverse barometer effect of the atmospheric tide by 2 h 25 min, or 1·26 rad. This is reasonably close to the observed phase lag of 1·38 rad. for the S_2 gravitational tide, suggesting that the ocean responds to the atmospheric pressure wave in much the same way. At the same time there must be direct radiational effects on the oceans, for the pressure amplitude in the tropics is 1·2 mb, and the gravitational admittance is only 0·62. The response to the atmospheric S_2 tide must not be confused with the response of sea level to *random* pressure variations at 2 c/d, for these have much larger spatial wavenumbers, and little spatial coherence. According to Munk & Bullard (1963) the sea-level response to the random variations is quasi-static.

6. Prediction variance

(*a*) *Tidal predictions*

Table 1 summarizes the observed, predicted, and residual variances of Honolulu sea level $\zeta(t)$. Convolutions of species 0 were computed from a 19 y 12-hourly series derived by low-passing $\zeta(t)$ with 0·5 c/d cutoff. Other species refer to the 19×355 d of 3-hourly series mentioned previously. The first row for each species shows the results for a response method with a maximum number of input variables; subsequent rows are for optimum predictions when certain variables are successively dropped. Weights corresponding to the top line for

each species in table 1 are listed in table 2. The lumped analysis leading to the smooth admittance curves refer to these weights.

In species 0, the radiational potentials marked with a prime are

$$\left.\begin{aligned} \alpha_1^{0\prime}(t) &= (365{\cdot}242/2\pi)\,[\alpha_1^0(t+\tfrac{1}{2}^d)-\alpha_1^0(t-\tfrac{1}{2}^d)],\\ \text{and}\qquad \alpha_2^{0\prime}(t) &= (365{\cdot}242/4\pi)\,[\alpha_2^0(t+\tfrac{1}{2}^d)-\alpha_2^0(t-\tfrac{1}{2}^d)].\end{aligned}\right\} \qquad (6{\cdot}1)$$

TABLE 1. HONOLULU PREDICTION VARIANCES FOR 1938–1957

species m	method	variables†	no. of station constants	variances (cm^2) observed‡ $\langle\zeta^2\rangle_m$	predicted σ_m^2	residual $\sigma^2_{\text{min.}}$	ratio $\sigma^2_{\text{min.}}/\langle\zeta^2\rangle_m$
0	response	a_2^0 (0, ±1), α_1^0, $\alpha_1^{0\prime}$, α_2^0, $\alpha_2^{0\prime}$	7	23·16	10·20	12·96	0·560
		As above, without a_2^0 (±1)	5	—	10·02	13·14	0·567
		α_1^0, $\alpha_1^{0\prime}$, α_2^0, $\alpha_2^{0\prime}$	4	—	9·64	13·52	0·584
		α_1^0, $\alpha_1^{0\prime}$	2	—	8·59	14·57	0·629
	harmonic	*Sa*, *Ssa*	4	—	8·72	14·44	0·624
1	response	c_2^1 (0, ±1, ±2, ±3), c_3^1 (0±1), χ_1^1, χ_2^1, $\bar{\zeta}.c_2^1$	26	154·78	154·70	0·08	0·0005
		As above, without χ_1^1, χ_2^1, $\bar{\zeta}.c_2^1$	20	—	154·63	0·15	0·0010
		c_2^1 (0, ±1, ±2)	10	—	154·61	0·17	0·0011
	harmonic	2*Q*, *Q*, *ρ*, *O*, *M*, *P*, *S*, *K*, *J*, *OO*	20	—	154·38	0·40	0·0026
2	response	c_2^2(0, ±1, ±2, ±3), c_3^2 (0, ±1), χ_2^2, $\bar{\zeta}.c_2^2$	24	157·63	157·50	0·13	0·0008
		As above, without $\bar{\zeta}.c_2^2$	22	—	157·40	0·23	0·0015
		c_2^2 (0, ±1, ±2, ±3), c_3^2 (0, ±1)	20	—	157·37	0·26	0·0016
		As above, without c_3^2 (±1)	16	—	157·35	0·28	0·0018
		c_2^2 (0, ±1, ±2)	10	—	157·30	0·33	0·0021
	harmonic	2*N*, *μ*, *N*, *ν*, *M*, *L*, *S*, *K*	16	—	157·11	0·52	0·0033
3	response	c_3^3 (0, ±1)	6	0·061	0·008	0·053	0·87
		c_3^3	2	—	0·008	0·053	0·87
total‡	response	all variables listed above	63	355·19	322·41	32·78	0·0923
	response	minimum number of variables listed above	24	—	320·51	34·68	0·0976
	harmonic	minimum number of variables	40	—	320·21	34·98	0·0985

† For example, c_3^1 (0, ±1) designates the six variables a_3^1 $(t-\Delta\tau)$, a_3^1 (t), a_3^1 $(t+\Delta\tau)$ b_3^1 $(t-\Delta\tau)$, b_3^1 (t), b_3^1 $(t+\Delta\tau)$. In all cases $\Delta\tau = 2$ d. Variables without parentheses were used with unlagged t only. χ_n^m refers to the radiational potentials $\alpha_n^m + i\beta_n^m$.

‡ The 'observed variances' are the energies of $\zeta(t)$ in the frequency ranges (0 to 4 c/m) (1 c/ld ±4 c/m), (2 c/ld±4 c/m), (3 c/ld±2 c/m), respectively. The 'total' observed variance is the overall variance of the lowpassed series $\zeta(t)$, including inter-tidal noise.

TABLE 2. HONOLULU WEIGHTS

variable	s	u_s	v_s	variable	s	u_s	v_s
a_2^0	1	−0·163524	—	c_2^2	3	−0·032468	−0·050293
	0	0·078005	—		2	−0·238275	0·292670
	−1	−0·089109	—		1	0·728548	−0·014861
α_1^0	0	−4·94637	−8·87672†		0	−0·505637	−0·853476
α_2^0	0	−11·99387	−13·50501†		−1	−0·004338	0·850862
c_2^1	3	0·015010	0·035523		−2	0·326582	−0·381108
	2	−0·035527	−0·072475		−3	−0·140442	0·033328
	1	0·229742	0·101201	c_3^2	1	−0·533411	−0·640720
	0	0·067604	−0·499019		0	0·141800	0·729601
	−1	−0·037543	0·218337		−1	0·264934	−0·092149
	−2	0·056136	−0·094427	χ_2^2	0	−1·98122	−1·36855
	−3	−0·018781	0·017824	$\bar{\zeta}c_2^2$	0	−0·00023	−0·00102
c_3^1	1	−0·402419	0·202837	c_3^3	1	0·007453	−0·240591
	0	0·394974	−0·254192		0	−0·101228	0·127434
	−1	−0·150418	0·107273		−1	0·053084	0·027965
χ_1^1	0	0·15069	−0·09649				
χ_2^1	0	−0·69386	1·58026				
$\bar{\zeta}c_2^1$	0	−0·00314	−0·00005				

† For the zonal radiational harmonics, v_0 refers to $\alpha_1^{0\prime}$, $\alpha_2^{0\prime}$, equation (5·1).

Since α_1^0 and α_2^0 are almost periodic functions at 1 c/y and 2 c/y respectively (see their spectra in figure 8), the functions defined in (6·1) are approximately their time-derivatives. They are included to accommodate fairly large phase lags arising from thermal inertia, which, unlike gravitational inertia, is important even at such low frequencies. We could have used instead terms like $\alpha_1^0(t-91^d)$ but such a large time lag is awkward to handle.

In the frequency band 0 to 4 c/m (strictly $\frac{1}{19}$ c/y to 4 c/m) we must expect a large prediction error from the high noise level. In fact, the residual variance is 56 % of the observed variance. Without any gravitational inputs the residual is 63 %, and so from a point of view of practical prediction the gravitational terms are hardly worth keeping.

The constants used for harmonic prediction were taken from International Hydrographic Bureau Special Publication no. 26, sheet 649. They were derived from 4 years of sea-level records except for *Sa* and *Ssa*, which were derived from 30 years of monthly mean levels. Harmonic prediction based on *Sa* and *Ssa* (hence four-station constants†) gives a residual error of 14·4 cm^2. The response method with the same number of station constants gives 13·5 cm^2; with seven constants it gives 13·0 cm^2 and with two constants 14·6 cm^2. So the response prediction does about as well as harmonic prediction with half the station constants, but neither method does very well.

In species 1 and 2 the advantage of the response method is more pronounced, but now both methods do very well. For species 1 the harmonic method with 20 station constants has a residual of 0·4 cm^2 as compared to the observed variance 154·8 cm^2; the response method with half the station constants has half the residual variance.‡

The variables $\overline{\zeta c_2^m}$ are nonlinear terms to study the interaction between the leading gravitational potential and low-frequency ($< 0{\cdot}5$ c/d) sea level.§ In this manner we had hoped to account for the cusp energies of order 0·1 cm^2 at K_1 and 1 cm^2 at M_2 (figures 3 and 4). In fact the cusp energies were not significantly reduced (see § 9 for further discussion). The input $\overline{\zeta c_2^m}$ could serve also to predict the result of line-line interactions such as $Ssa-M_2$, but these are negligible anyway.

The reduction in σ_2^m when a term is excluded is not necessarily a good test of its importance. For example, the weights derived for the radiational potential χ_2^2 ($u_0 = -1{\cdot}98$, $v_0 = -1{\cdot}37$), when multiplied by the appropriate latitude factor, agree very well with the radiational energy of about 1·6 cm^2 deduced from the sequential analysis (§ 5). The fact that its omission causes σ_2^2 to fall by as little as 0·03 cm^2 is due to a readjustment of the weights of the gravitational terms to compensate for the absence of χ_2^2. In effect the estimate of gravitational admittance becomes distorted in the solar frequency group to allow partially for the apparent anomaly. This self-compensation for faulty (or incomplete) input functions does not apply to cusps since these occupy largely non-tidal parts of the spectrum.

The response to species 3 is ineffective in prediction because the energy of the ter-diurnal

† Constants for *Mm* and *Mf* are not given in the published list, but they would be unlikely to improve the harmonic prediction any more than α_2^0 does in the response prediction.

‡ This advantage applies even though we used a program (devised by G. W. Groves) which infers some harmonic constants, not actually supplied, from strong neighbouring lines. Thus, our harmonic prediction involves more terms than are quoted in table 1.

§ For the purpose of computing tide prediction tables, the use of recorded sea level $\hat{\zeta}(t)$ among the input functions would of course be ruled out.

tides is very small as compared with the continuum energy (which is itself very low). No ter-diurnal harmonic constants are given in the published list.

In assessing the overall prediction variances at the bottom of table 1, we have to remember that the total variance of $\zeta(t)$ contains also the energy between the bands of tidal frequency, especially in the range between species 0 and 1. Also, the efficiency of the diurnal and semi-diurnal predictions are to some extent marred by the inefficiency at species 0. The noise level at Honolulu is less than in places which experience stronger weather. Yet compared to the exceptionally low tides the noise level is rather high, so that the residual ratio, about 9 % for the response, 10 % for harmonic predictions, is higher than the corresponding ratio for typical ports.

(*b*) *Self prediction*

We now consider the variation in sea level after removal of all tidal effects. The variance of the residual 'sea level' in the frequency band 0 to 0·5 c/d is 26·6 cm^2. Imperfections in the removal of gravitational and radiational components are negligible as compared to this residual, and any significant improvement in prediction must depend on some means of predicting the residual.

Two procedures (and their combination) suggest themselves: (i) to include some meteorological variables $c_k(t)$ as additional input functions into the prediction formulae (see § 10); and (ii) to make use of the past tide record itself as an input.

Figures 9 and 10 show the power spectrum and auto-covariance of the residual sea level at Honolulu. Nearly all the contribution to the variance comes from frequencies below 12 c/y and, accordingly, the auto-covariance remains large for lags up to 1 month. With this degree of persistence one expects useful self-predictions for periods up to 1 month.

For a prediction τ_s days in advance we may write

$$\hat{\zeta}(t) = \sum_{s=1}^{S} w_s \zeta(t-\tau_s),$$

with the prediction weights, w_s, to be determined by the condition that the residual variance be a minimum. The problem is closely analogous to prediction using the tide potential as input function, except that in the present case the input is the (real) process $\zeta(t)$ itself, and that only its past values are permissible.

The results are shown in figure 9. The series analysed consisted of residual $\zeta(t)$ sampled at $\frac{1}{2}$ d intervals over a period of 19 y. For any given prediction time of τ_s days, we chose the lags τ_s, $1{\cdot}25\tau_s$, $1{\cdot}50\tau_s$ in one model, and a single lag τ_s in a second model. The improvement of the triple lag model over the single lag model is surprisingly small. (Prediction with τ_s, $1{\cdot}50\tau_s$, $2\tau_s$ led to the same conclusion.) The result is reminiscent of a Markov sequence for which optimum prediction is based only on the most recent observed value, a knowledge of values at earlier times being of no use whatsoever in improving the prediction.

We have also attempted to fit the observed spectrum and covariance by a class of functions which includes the Markov process as a special case. The best fit was obtained for the Markovian case. Apparently the prediction of residual sea level, as so many geophysical processes, is possible only in this limited sense.

For the single lag model the predicted sea level is

$$\hat{\zeta}(t) = w_s \zeta(t-\tau_s), \qquad (6{\cdot}2)$$

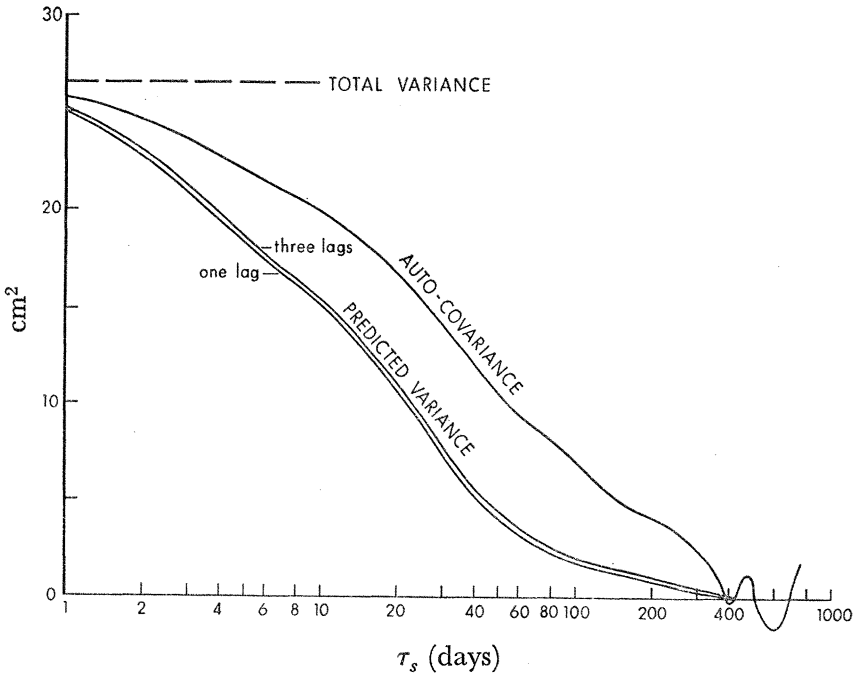

FIGURE 9. Auto-covariance curve for Honolulu sea level after removal of energy above $\frac{1}{2}$ c/d and of low-frequency gravitational and radiational tides. The lower curves are the self-predicted variances, σ_s^2, as functions of the prediction time τ_s, for a single lag τ_s, and for the three lags τ_s, $1{\cdot}25\tau_s$, $1{\cdot}50\tau_s$, respectively.

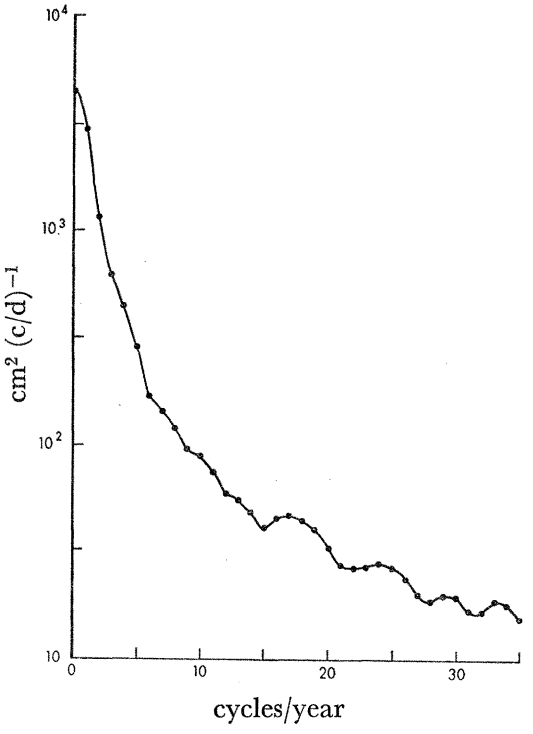

FIGURE 10. Power spectrum of the residual (tide-free) Honolulu sea level from 1938 to 1957.

where
$$w_s = \frac{\langle \zeta(t)\, \zeta(t-\tau_s)\rangle}{\langle \zeta^2(t)\rangle} \tag{6·3}$$
is the auto-correlation. The associated variances are:

observed	predicted	residual	residual/observed
$\langle \zeta^2 \rangle$	$w_s^2 \langle \zeta^2 \rangle$	$(1-w_s^2)\langle \zeta^2 \rangle$	$1-w_s^2$

(6·4)

Self-prediction 14 days in advance reduces the variance from 26·6 cm^2 to half this value. For 1 month the reduction is small, from 26·6 cm^2 to 26·6 − 7·6 = 19 cm^2, and for 1 year the reduction is utterly negligible. Self-prediction is then of no use in improving published Honolulu tide tables. But it is conceivable that records from digital tide gauges can be removed on (say) 24 January, promptly analysed to give 'improved February tide' predictions, and be distributed prior to 1 February to interested parties. Whether this is worthwhile is an operational question.

So far we have dealt with the prediction of instantaneous sea level τ_s days in advance. A prediction of the mean monthly or mean annual sea level can of course be given with greater precision, because smoothing reduces the high-frequency components of the spectrum and extends the covariance to larger lags. Smoothing times and prediction times are independent variables; in the special case that these are equal (e.g. monthly means predicted 1 month ahead) we have, for a smoothed Markov process,
$$\overline{w}_s = \frac{2\sinh^2(\frac{1}{2}\gamma\tau_s)\, e^{-\gamma\tau_s}}{\gamma\tau_s + e^{-\gamma\tau_s} - 1} = 1 - \tfrac{2}{3}\gamma\tau_s + \dots$$
as compared to $w_s = e^{-\gamma\tau_s}$ for the unsmoothed process (Munk 1960). The prediction time is lengthened by only 50 % for the smoothed process.

7. Nonlinear perturbations

It is well known that nonlinear effects, particularly those associated with shallow water, can lead to significant distortions of the tidal profile. The departure from linearity varies greatly from place to place, from a small perturbation as at San Francisco to a near-bore condition as at Avonmouth. Accordingly we may divide ports into three classes, depending on whether:

(i) tides are virtually linear;
(ii) tides are analysable by perturbations up to second or third order;
(iii) perturbations are divergent or otherwise unmanageable.

Honolulu typifies (i); we now consider category (ii), with Newlyn as example. Category (iii) is outside the scope of this paper, but we shall comment in § 10.

Nonlinear interactions are accommodated in harmonic prediction by allowing constituents at sums and differences of the frequencies of the main linear constituents. However, the number of additional constituents so required increases rapidly with increasing nonlinearity, (even when allowing for multiple nonlinear constituents; e.g. those whose frequencies coincide with linear constituents), and the f, u modulating scheme becomes inaccurate. Perturbations to the response method are better manageable.

The bilinear prediction can be written

$$\hat{\zeta}^{\mathrm{II}}(t) = \sum_i \sum_s w_{is}\, c_i(t-\tau_s) + \sum_{ij} \sum_{ss'} w_{ijss'}\, c_i(t-\tau_s)\, c_j(t-\tau_{s'}), \tag{7·1}$$

where $c_i(t)$ represents the complex linear input functions for any m, n, whether gravitational, radiational or otherwise. In the double summation, the product $c_i(t-\tau_s)\, c_j(t-\tau_{s'})$ can be of various types:

(i) first order predictions: $\hat{\zeta}^{\mathrm{I}}(t-\tau_s)\, \hat{\zeta}^{\mathrm{I}}(t-\tau_{s'})$;
(ii) various linear inputs: $c_i(t-\tau_s)\, c_j(t-\tau_{s'})$;
(iii) recorded and linear inputs: $\zeta(t-\tau_s)\, c_i(t-\tau_{s'})$.

In procedure (i) we first evaluate w_{is} to obtain the linear prediction $\hat{\zeta}^{\mathrm{I}}(t)$ according to (4·17). In a second step, $\hat{\zeta}^{\mathrm{I}}(t)$ serves as input function into (7·1), and the linear weight w_{is} are re-evaluated together with $w_{ijss'}$ in a combined linear-nonlinear matrix inversion.† This procedure has the advantage that linear modifications of the tides are already allowed for in the bilinear input functions, and accordingly the biadmittances can be expected to be smoother than for (ii), and require fewer bilags. For (ii) the biweights have to absorb both linear and quadratic effects, but there is the advantage that linear and nonlinear weights are evaluated in a single step. (iii) is useful for research on nonlinear interactions; as a predictor it is limited to the smallest value of τ_s.

Whichever of the foregoing schemes is adopted, the bilinear input can be written as a (complex) product of $c_1^m(t)$ and $c_j^{m'}(t)$, representing various (complex) linear functions belonging to species m and m', with $m \geqslant m'$. We use

$$c_{ij}^{m+m'} = c_i^m\, c_j^{m'}, \quad c_{ij}^{m-m'} = c_i^m\, c_j^{m'*} \tag{7·2}$$

for a shorthand notation to designate overtides of species $m \pm m'$. The associated biadmittances are given by the two-dimensional Fourier transforms

$$Z(f,f') = \sum_{s=0}^{S} \sum_{s'=0}^{S'} w_{ss'} \exp\left[-2\pi \mathrm{i}(f\tau_s \pm f'\tau_{s'})\right]. \tag{7·3}$$

At the discrete frequencies $f = r/355$ c/d, $f' = r'/355$ c/d, the foregoing expression equals precisely the estimate

$$Z_{rr'} = H_{r\pm r'}/G_r\, G_r$$

derived from the one-dimensional Fourier transforms $H_{r\pm r'}, G_r, G_{r'}$ of $\zeta^{m\pm m'}$, c^m, $c^{m'}$, respectively.

Trilinear convolutions can be dealt with by an extension of the foregoing analysis. We used only the unlagged complex interaction $\hat{\zeta}^{\mathrm{III}} = \hat{\zeta}^{\mathrm{I}} \hat{\zeta}^{\mathrm{I}} (\hat{\zeta}^{\mathrm{I}})^*$ between species 2 predictions.

8. Results for Newlyn

(a) *Procedure and choice of variables*

The following discussion deals with linear as well as nonlinear interactions. Newlyn ($\theta = 39^\circ 54'$, $\lambda = -5^\circ 34'$) is a typical example of nonlinear category (ii). While better exposed to the North Atlantic Ocean than most European ports, it is on a continental shelf some 300 km wide and typically 100 m deep, and this causes an appreciable but not excessive amount of shallow-water distortion.

† The matrix formalism in §4 (*g*) can readily be adopted to include nonlinear terms.

We analysed precisely the same 19×355-day period as for Honolulu, but in a somewhat different way. The sequential analysis adopted for Honolulu is less effective here because of the many multiple components (§ 4 (*e*), multiple component (ii)). We therefore carried through only the lumped analysis, including bilinear and trilinear terms. Choice of non-linear variables is simplified by the strong dominance of semi-diurnal tides at Newlyn. Products with $m = m' = 1$ or 3 can be ignored, so the only inputs we need consider are c^{2-2}, c^{2-1}, c^{2+0} and c^{2+2-2}, c^{2+1}, c^{2+2} for species 0, 1, 2, 3, 4, respectively. The procedure of solving the weight matrices was as follows. First a smoothed series with 4 c/d cutoff, 8 values per day, was produced as for Honolulu, and all 19×355 days processed to give weights for species 1, 2 and 3. The convolution on c_2^2 (with other variables eliminated) gave the first-order prediction $\hat{\zeta}^{\mathrm{I}}$ for species 2, which served as bilinear inputs $(\hat{\zeta}^{\mathrm{I}})^{2\pm2}$ to species 4 and 0. In the subsequent bilinear analysis for species 0, we used 19 y of a twice-daily smoothed series with 0·5 c/d cutoff; for species 4 we used the original hourly readings of $\zeta(t)$, but for only three 355-day periods, at 6 y intervals.

The only published list of harmonic constants for Newlyn at present is I.H.B., sheet no. 1, which is based on only 6 months' analysis of data in 1915. We consider it an unfair test of the harmonic prediction to use this list, and therefore computed our own set of harmonic constants (table 5) from a 710 day record with central date 13 April 1948. *Sa* and *Ssa* were computed from the whole 19 y of data.

(*b*) *Prediction variances*

Tables 3 and 4 summarize the results of the lumped analysis for Newlyn. The residual variance in species 0 is much higher than at Honolulu because of the more severe weather at the higher latitude.

For species 0 we experimented with types (i) and (ii) of bilinear inputs (§ 7); the former give $(\hat{\zeta}^{\mathrm{I}})^{2-2}$ and are based on first-order prediction, the latter give a_2^{2-2} arising from the linear input functions. The two types of bilinear input do about equally well. Here it is remarkable how small the difference-frequency interaction is, of order 1 cm^2, as compared to 100 cm^2 for the sum-frequencies producing species 4. As another measure of this disparity we may compare the amplitudes of the harmonic constituents *MSf* and MS_4, namely 1·4 7·4 cm respectively. The disparity can be accounted for by shallow water wave theory (cf. Lamb, 1932 p. 281). In a perturbation expansion for free waves progressing over a shelf of constant (shallow) depth h, the first two terms are

$$\left.\begin{aligned} \zeta^{\mathrm{I}}(x,t) &= \sum_p r_p \, \mathrm{e}^{\mathrm{i}\chi_p}, \quad \chi_p = \sigma_p\left(t - \frac{x}{\sqrt{(gh)}}\right), \\ \zeta^{\mathrm{II}}(x,t) &= \zeta^{\mathrm{I}}(x,t) + \frac{3}{8}\sqrt{\left(\frac{g}{h^3}\right)} \sum_p \sum_q r_p r_q [(\sigma_p+\sigma_q)\exp\{\mathrm{i}(\chi_p+\chi_q+\tfrac{1}{2}\pi)\} + (\sigma_p-\sigma_q)\exp\{\mathrm{i}(\chi_p-\chi_q+\tfrac{1}{2}\pi)\}] \end{aligned}\right\} \tag{8·1}$$

and we should expect the amplitude of *MSf* to be about (2 c/m)/(4 c/d) = 0·02 times that of MS_4. At c/y resolution, *MSf* is in fact scarcely distinguishable from noise, so its true amplitude may well be much less than 1·4 cm.

For species 1 we included both types (ii) and (iii) of bilinear inputs, c_2^{2-1} and $\overline{\zeta}.c_2^1$, where $\overline{\zeta}$ is the unlagged recorded sea level low-passed to 0·5 c/d. Neither type contributes appreciable energy.

Table 3. Newlyn prediction variances

species m	method	variables†	no. of station constants	variances (cm^2) observed $\langle\zeta^2\rangle_m$	predicted σ_m^2	residual $\sigma_{\min}^2$	ratio $\sigma_{\min}^2/\langle\zeta^2\rangle_m$
0	response	a_2^0 (0, ±1), α_1^0, $\alpha_1^{0\prime}$, α_2^0, $\alpha_2^{0\prime}$, a_2^{2-2} (0, 0), (0, ±1)	10	155	20	135	0·871
		as above, with $(\hat{\zeta}^{\mathrm{I}})^{2-2}$ instead of a_2^{2-2}	8	—	19	136	0·877
		as above, without bilinear terms	7	—	18	137	0·865
	harmonic	*Sa*, *Ssa*, *MSf*, *Mf*	8	—	16	139	0·897
1	response	c_2^1 (0, ±1, ±2), c_3^1, χ_1^1, χ_2^1, $\overline{\zeta}\, c_2^1$, c_2^{2-1} (0, 0), (−1, 0), (0, −1), (1, 0), (0, 1)	28	40	38	2	0·050
		c_2^1 (0, ±1, ±2)	10	—	37	3	0·075
	harmonic	see table 5	22	—	37	3	0·075
2	response	c_2^2 (0, ±1, ±2, ±3), c_3^2 (0, ±1), χ_2^2, $\overline{\zeta}\hat{\zeta}^{\mathrm{I}}$, $\hat{\zeta}^{\mathrm{I}}\hat{\zeta}^{\mathrm{I}}$ $(\hat{\zeta}^{\mathrm{I}})$	26	17060	17051	9	0·0005
		As above, without nonlinear terms	22	—	17029	31	0·0019
		c_2^2 (0, ±1, ±2, ±3)	14	—	17020	40	0·0023
	harmonic	see table 5	24	—	17055	5	0·0003
3	response	c_3^3 (0, ±1), c_2^{2+1} (0, 0), (±1, 0), (0, ±1)	16	1·2	0·7	0·5	0·42
		c_3^3 (0, ±1)	6	—	0·6	0·6	0·50
	harmonic	*M*, *MK*, *SK*	6	—	0·6	0·6	0·50
4	response	c_2^{2+2} (0, 0), (−1, −1), (0, ±1), (1, ±1)	12	103	102	1	0·01
		$(\hat{\zeta}^{\mathrm{I}})^{2+2}$	2	—	101	2	0·02
		c_2^{2+2}	2	—	76	27	0·26
	harmonic	*MN*, *M*, *MS*, *MK*, *S*	10	—	100	3	0·03
total	response	all variables listed above	92	17400	17212	188	0·011
	response	minimum number of variables listed above	39	—	17177	223	0·013
	harmonic	all variables listed above	70	—	17209	191	0·011

† The symbolism is the same as in table 1, except for bilinear terms. a_2^{2-2} (0, 0) (0, ±1) designates the three variables $a_2^{2-2}(t, t-\Delta\tau)$, $a_2^{2-2}(t, t)$, $a_2^{2-2}(t, t+\Delta\tau)$. a_2^{2-2} without parentheses designates $a_2^{2-2}(t, t)$. $(\hat{\zeta}^{\mathrm{I}})^{2-2}$ represents the difference frequencies of the unlagged complex linear predictions for species 2.

Table 4. Newlyn weights

variable	s	u_s	v_s
a_2^0	1	0·17279	—
	0	−0·06111	—
	−1	0·19196	—
α_1^0	0	−10·10901	−9·55470
α_2^0	0	1·02773	25·51777
$(\hat{\zeta}^{\mathrm{I}})^{2-2}$	0, 0	$4{\cdot}63\times10^{-6}$	—
c_2^1	2	0·25529	0·23613
	1	−0·47527	−0·37177
	0	0·37520	0·55067
	−1	−0·17257	−0·47404
	−2	−0·00802	0·18129
c_3^1	0	0·05493	1·22219
χ_1^1	0	−0·22171	0·07908
χ_2^1	0	7·11996	4·56625
$\overline{\zeta}.c_2^1$	0	−0·00006	0·00012
c_2^{2-1}	0, 0	−0·00355	−0·00328
	−1, 0	0·00153	0·00041
	0, −1	0·00047	0·00065
	1, 0	−0·00017	0·00229
	0, 1	0·00109	−0·00053
$(\hat{\zeta}^{\mathrm{I}})^{2+2}$	0, 0	-61×10^{-6}	368×10^{-6}

variable	s	u_s	v_s
c_2^2	3	0·68689	−1·77475
	2	−7·91864	2·76338
	1	13·48524	7·19030
	0	−9·42739	−20·60248
	−1	−5·18210	17·29659
	−2	8·28395	−4·86726
	−3	−2·55434	−0·84152
c_3^2	1	0·46432	3·35623
	0	3·57749	−2·78616
	−1	−1·73939	0·25917
χ_2^2	0	22·42819	24·78512
$\overline{\zeta}.\hat{\zeta}^{\mathrm{I}}$	0	−0·00025	−0·00017
$\hat{\zeta}^{\mathrm{I}}.\hat{\zeta}^{\mathrm{I}}.(\hat{\zeta}^{\mathrm{I}})$*	0	$-2{\cdot}16\times10^{-6}$	$-2{\cdot}18\times10^{-6}$
c_3^3	1	0·92303	0·76366
	0	−0·64915	−1·30128
	−1	−0·91930	0·15372
c_2^{2+1}	0, 0	−0·00035	0·00029
	−1, 0	−0·00025	−0·00011
	0, −1	0·00028	−0·00013
	1, 0	0·00025	−0·00016
	0, 1	0·00004	0·00022

For species 2 we used a bilinear term of type $\overline{\zeta}\hat{\zeta}^{\mathrm{I}}$ and a trilinear term $\hat{\zeta}^{\mathrm{I}}\hat{\zeta}^{\mathrm{I}}(\hat{\zeta}^{\mathrm{I}})^*$. The interaction $\overline{\zeta}\hat{\zeta}^{\mathrm{I}}$ produces cusps of the order of 1 cm^2, but these account for only a small fraction of the recorded cusp energy. Other types of bilinear inputs are inadequate, since $a_2^0, \alpha_1^0, \ldots$ contribute so little to the low frequency sea level. We note that the trilinear interaction contributes significantly to the prediction variance, since it drops by 22 cm^2 when the term is omitted.

Prediction variance for species 2 is reduced by some 10 cm^2 by neglecting χ_2^2. This is not a true measure of the semi-diurnal radiation because the gravitational convolution adapts itself somewhat to the missing input. The weights associated with χ_2^2 represent a 2 c/d constituent of 19 cm amplitude lagging the Sun's transit by 10 h 24 min (5·45 rad). The equivalent lag on the inverse atmospheric tide is 6 h 24 min = 3·35 rad, and compares reasonably with that of the c_2^2 convolution. 19 cm may seem to be remarkably large for a non-gravitational tide, but bearing in mind that the admittance to the P_2^2 spherical harmonic is of order 15 at Newlyn, compared with 0·6 at Honolulu (where we got 1·8 cm radiational S_2), we see that it is quite reasonable.

TABLE 5. HARMONIC CONSTANTS USED FOR NEWLYN

constituent	H	κ	constituent	H	κ	constituent	H	κ
Sa	5·48	223·4	$2Q_1$	0·43	262·1	MNS_2	1·09	136·0
Ssa	1·57	111·4	σ_1	0·36	268·1	$2N_2$	5·87	097·4
MSf	1·44	158·1	Q_1	0·91	291·9	μ_2	5·16	159·5
Mf	1·35	223·3	ρ_1	0·45	307·1	N_2	32·21	103·3
M_3	0·97	006·0	O_1	5·29	339·1	ν_2	7·92	098·1
MK_3	0·67	274·2	M_1	0·33	319·0	M_2	171·05	123·2
SK_3	0·18	070·0	π_1	0·33	099·5	λ_2	3·75	117·2
MN_4	4·20	117·4	P_1	2·39	097·0	L_2	8·03	131·8
M_4	10·28	145·1	S_1	0·23	014·4	T_2	3·01	159·6
MS_4	7·37	198·1	K_1	6·45	103·6	S_2	57·76	165·9
MK_4	2·26	204·1	J_1	0·22	075·3	K_2	16·78	163·3
S_4	1·03	259·7	—	—	—	$2SM_2$	2·09	007·5

H (cm) and κ (degrees) are in the conventional notation.

For species 4 we note that a bilinear input $(\hat{\zeta}^{\mathrm{I}})^{2+2}$ gives almost as large a predicted variance with unlagged t as c_2^{2+2} with 6 lag-pairs, and does considerably better than $c_2^{2+2}(0, 0)$ alone. This is because the linear admittance for species 2 is rather irregular, and so its product cannot be well simulated with just one lag pair. For the unlagged weight, $\arg w$ is close to the value $\frac{1}{2}\pi$ suggested by (1). Assuming 300 km for the shelf width x, then $|w|$ is consistent with a uniform depth of 42 m. The true mean depth is about 100 m, but the negative power of h in (1) will give greater weight to the shallower parts of the shelf.

We see from table 5 that the neighbouring constituents $2N_2$ and μ_2 differ in phase by 62°, presumably due to the multiple components $2N_2$ and $2MK_2$, μ_2 and $2MS_2$ (but a jitter (§ 5 (*c*)) may be partly responsible). Since $2N_2$ and μ_2 differ in frequency by only 2 c/y, our smoothed admittances cannot adapt to such rapid changes, and so they become inaccurate for both constituents, unless the triple interaction terms are included.

In all species except 2, predictions by the response method are slightly better than by the harmonic method, even with a lesser number of constants.

With regard to the overall picture, we note that at Newlyn the energy of the low frequency

residual is five times that at Honolulu, and the tidal energy fifty times as large. As a result the overall residual *ratios* are less at Newlyn than Honolulu, 1 % as compared with 10 %.

On subtracting low frequency tidal effects from the low-passed $\zeta(t)$ with cut-off at 0·5 c/d we obtained a residual series with variance 148 cm^2. Autocovariances and self-prediction variances for this series are shown in figure 11. The persistence is less at Newlyn because of the larger contribution by 'weather' to the continuum at 0·1 to 0·2 c/d (cf. figure 12, panel 5 with figure 1, panel 3). Consequently, the self-predicted variance for Newlyn falls off much more rapidly with prediction time and is negligible for a 10 day prediction.

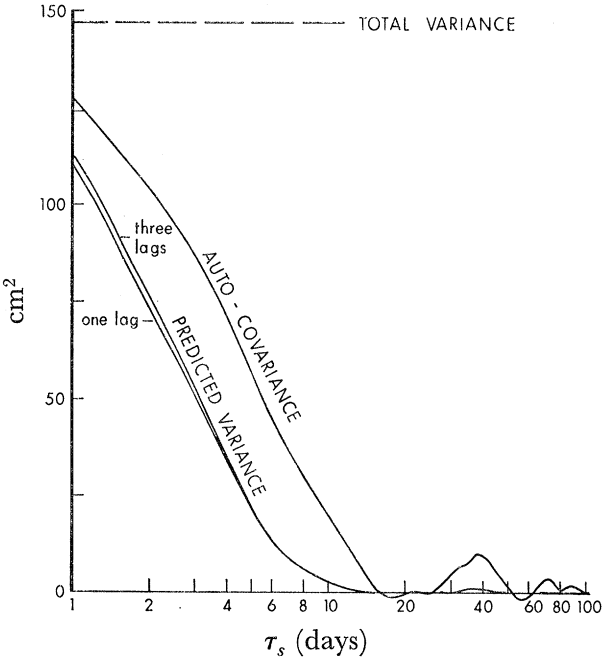

FIGURE 11. Auto-covariance and self-prediction curves for Newlyn. Description as in figure 9.

(*c*) *Spectral composition and admittances*

The spectrum of three linear inputs was multiplied by the squared admittance corresponding to the response weights to give the output spectra in the top three panels of figure 12. Bispectra were computed and multiplied by the appropriate biadmittance, and the mean energies plotted in the fourth panel. The fifth panel is very similar to the third panels of figures 1 and 7, except that the residual energy is the mean energy of $\zeta(t)$ after subtraction of the vector sum of all four components shown above. All ensemble averages are over 19 y and 13 adjacent c/y harmonics.

The diagram does not allow for triple interactions, as these were computed at a later stage. Occasional bumps in the lesser groups of species 2, as well as irregularities in the P_2^2 admittances were removed when we allowed for triple interactions. Cusp-type residuals are conspicuous at species 2 and 4.

All the linear admittances to gravitational inputs are plotted in the bottom diagrams. P_3^1 was allowed only unlagged t, so the equivalent constant admittance is printed. The admittance curves for P_2^1 and P_2^2 are noticeably more wiggly than the corresponding curves

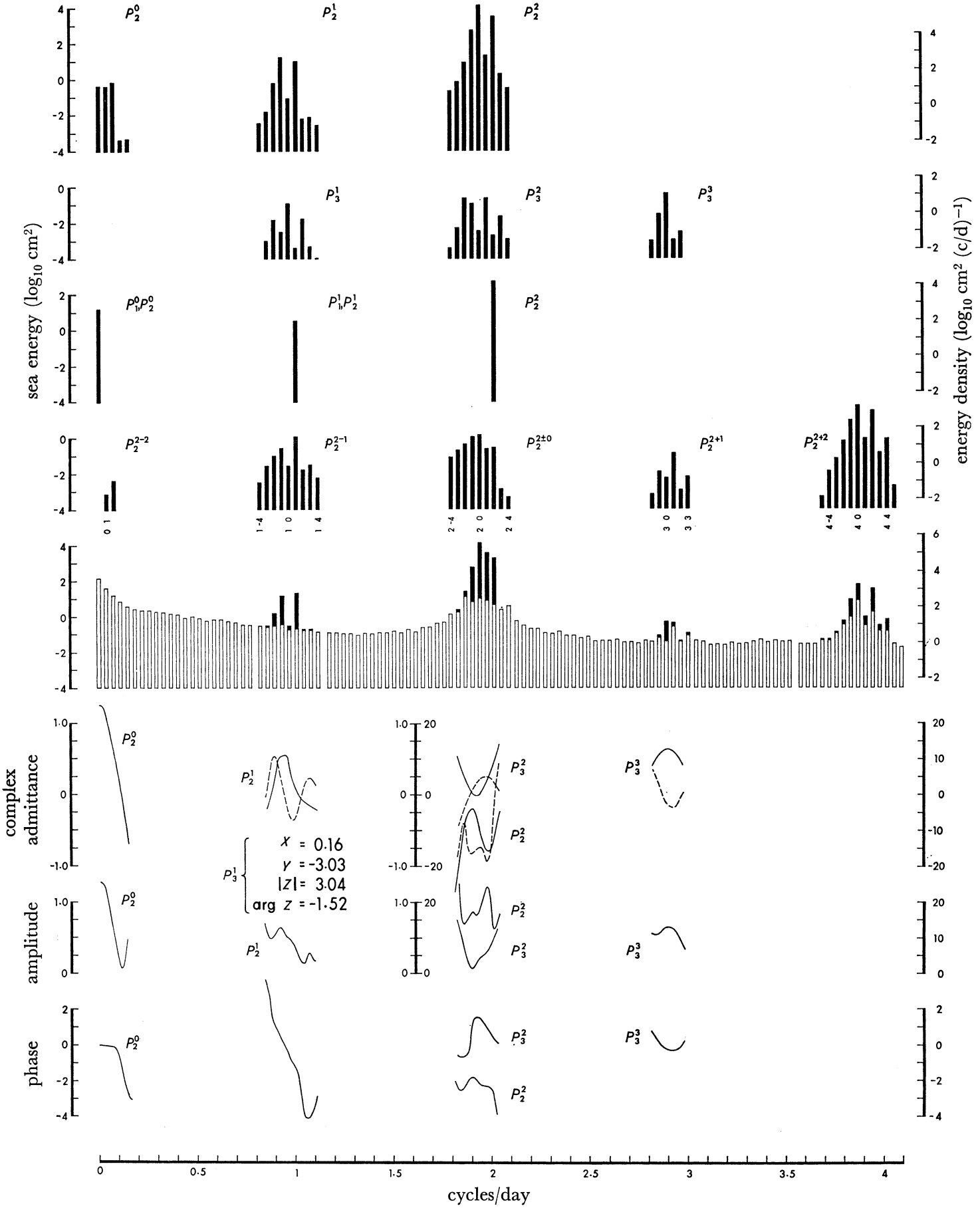

FIGURE 12. Newlyn tide spectra at 1 c/m resolution. The top four panels represent the sea spectrum due to (1) gravitational tides, degree 2, (2) gravitational tides, degree 3, (3) radiational tides, and (4) bilinear interaction. In the fifth panel, the total height of each column represents the observed sea spectrum, and the lower (unfilled) portion is the residual energy when the four components above have been subtracted. The lowest diagrams show the linear gravitational admittance functions derived from the response weights. Dashed curves are imaginary admittances, phase leads are in radians.

for Honolulu. The steep decrease of phase for P_2^1, about 34 rad (c/d), is remarkable. It implies that a smoother admittance would be obtained by using $c_2^1(t-5^d)$ instead of $c_2^1(t)$.

The isolated peak at (2 1) followed by a trough at the solar group (2 2) is reflected in the unusually large L_2 constituent and the fact that the radiational term accounts for a fair proportion of the S_2 constituent. (The true gravitational S_2 has amplitude 79 cm and phase $-146°$). It might be suspected that the trough at (2 2) is an analytical defect, allowing χ_2^2 to contribute too much to the group. That this is not so was proved by estimating the gravitational admittance directly from the purely lunar lines such as (2 2 0 0 1), which were also used for Honolulu. The resulting admittance

$$X = -12{\cdot}3, \quad Y = -3{\cdot}9, \quad |Z| = 12{\cdot}9, \quad \arg(Z) = -2{\cdot}83$$

compares favourably with the values

$$X = -13{\cdot}0, \quad Y = -5{\cdot}0, \quad |Z| = 14{\cdot}4, \quad \arg(Z) = -2{\cdot}82$$

from the admittance curve in figure 12 at the frequency of (2 2 0).

It is interesting to note that the admittances to P_3^2 and P_3^3 are, like the admittances to P_2^2, of order 10 in magnitude, even though their resulting energies are still very small. This, and the enhanced radiational effects, are presumably due to local shelf resonances in the range 2 to 3 c/d.

9. Jitter and cusps

The derivation of the port admittances now provides a challenge for interpreting these in terms of tidal dynamics and offshore topography. For Newlyn the admittances are surprisingly complex. At Honolulu the admittances are reasonably smooth, particularly when viewed at c/y resolution. But even then there appears to be a significant 'jitter' between values separated by 2 c/y. All tests to account for this in terms of bilinear interactions have failed, as also consideration of higher order terms in the lunar orbit theory, spherical harmonics of degree 3, Earth's oblateness, and statistical sampling.

The following hypothesis for jitter has occurred to us, and will require further study. The bottom drag on tidal currents, and the mechanism of the tide gauge† are associated with frictional effects of the form $\dot{\zeta}|\dot{\zeta}|$ which, being an odd function of ζ, will produce trilinear interactions without bilinear effects. Triple interactions between each strong line with P_1 and K_1, or with M_2 and S_2, will modify the weak constituents at 2 c/y separation, as observed. As supporting evidence, figure 4 shows a bump in the sea-level spectrum at (2 4 −4), corresponding to the trilinear constituent $2SM_2$. Subsequent trilinear analysis for Newlyn did in fact lead to a significant reduction in residual variance, and this strongly implies a corresponding reduction in jitter.

At Honolulu and Newlyn the continuum spectrum was found to rise sharply in the vicinity of the strong lines. The simplest explanation is the one proposed by Munk *et al.* (1965), that the cusps represent the sidebands due to the modulation of a carrier (the tides) by a low-frequency noise (the continuum at very low frequencies). Accordingly we expected significant bilinear coherences for the noise-line interaction $\bar{\zeta}c$. The computed bilinear coherences were insignificant. We have considered and rejected three possible explanations.

† This raises an interesting problem concerning optimum prediction of sea level as opposed to water level in the tide well.

(i) *The cusp is merely a result of some numerical defect in the computing procedure.* We generated an an artificial series of 355 days, consisting of a harmonic tide prediction plus a random 'noise' with the appropriate low-frequency enhancement. All dimensions corresponded roughly to the sea spectrum at Honolulu. The artificial record was analysed in the same manner as the Honolulu record. The noncoherent energy is virtually uniform in the neighbourhood of the strong tidal lines.

(ii) *The cusp energy is due to nonlinearity in the tide gauge itself*, as a result of clock errors or octopus tentacles in the orifice, etc. A year's record from a precision bottom-placed pressure recorder at La Jolla (Snodgrass 1964) yielded a cusp centred on group (2 0) of about 1 cm^2 energy, very much as at Honolulu.

(iii) *The cusp is due to global, rather than local, interaction*, so that there is no relation between the cusps and the *locally* recorded continuum near zero frequency. But then there should still be relations between cusps at two adjoining stations, and between the two sides of a cusp at a single station. We isolated the cusp spectra at c/y resolution from 7 y of simultaneous tide records at Honolulu and Kahalui (an island port about 100 km southeast of Honolulu), and computed cross-spectra and coherences. The energy of the cusp at Kahalui is about half that at Honolulu, although the tidal amplitudes are about the same. The cross-spectra at c/y resolution bear no uniform relation, and the coherence from ensemble averages extending over 7 record years and 19 neighbouring c/y harmonics centred on M_2 is practically zero. Since the separation of the ports is a small fraction of a tidal wavelength, we should expect high coherence under hypothesis (iii). In another test we examined separately the left and right sides of the cusp about M_2 at Hawaii. Upon demodulation, each the side bands was expected to carry approximately the same information. The test was negative.

At this time we have no convincing model. Toshitsugu Sakou & Gordon Groves (personal communication) have made the interesting suggestion that the cusp energy represents the small surface oscillations associated with internal tides; the spreading into cusps is to be associated with a modulation of the internal tides by the slowly varying thermal structure.

10. Further remarks concerning prediction

Ultimately the prediction scheme for a given port must depend upon the relative contribution from 'noisy' processes (processes with a continuous spectrum) and from nonlinear processes.

For noisy processes one is limited to *short range* predictions, depending on persistence. The prediction times might be of the following order: storm tides, 1 day; changes in level due to river runoff, 1 week; 'mean' sea level, 1 month. The appropriate formalism is

$$\hat{\zeta}(t) = \sum_i \sum_s w_{is} c_i(t-\tau_s) \qquad (10{\cdot}1)$$

where the i input processes $c_i(t)$ may include atmospheric pressure and wind at strategic locations, sea level at various ports (including the port in question, see § 6 *b* on self prediction), etc. The weights w_{is} are determined from past records by matrix inversion (§ 4 (*g*)). The problem is complicated by the fact that the input functions will in general be partially coherent with one another. Thus, the optimum weights w_{is} associated with any particular

input process will depend on what other processes are included. But all this can be sorted out. The principal task for a good short-range prediction of storm tides will be the establishment of a communications network to supply the appropriate input functions into a computer for 'real time' processing and prediction.

With regard to nonlinearity we have considered the cases of (i) Honolulu, linear prediction adequate; (ii) Newlyn, prediction should allow for bilinear and trilinear interactions; (iii) wildly nonlinear stations. For the last case, we plan to develop the response method to a high-order perturbation. We are also considering a method involving the concept of an 'equivalent deep-water port', a fictitious station so defined as to have tides identical with the actual port if nonlinear processes were lacking. The transformation from the predicted equivalent tide $\hat{\zeta}_e(t)$ to the predicted actual tide $\hat{\zeta}(t)$ is afforded by introducing delay and distortion terms:

$$\hat{\zeta}(t) = \alpha\hat{\zeta}_e(t-\tau), \tag{10·2}$$

with α and τ functions *not* of frequency, but of elevation $\hat{\zeta}_e(t)$ (as in the method of characteristics). The proposed development carries a step further the central concept of this paper: to replace the harmonic by a response scheme which avoids considerations of the splitting of each species into a spectral cluster. Here we propose to avoid even the decomposition into species as far as the nonlinear effects are concerned, with the assumption that the propagation of a tide across a shallow shelf depends only on the instantaneous elevation of water level at the outer edge.

Severe noisiness and nonlinearity tend to go together in shallow water ports, and one may contemplate a combination of the schemes sketched in this section. But it is by no means clear whether an iterative scheme can be devised which converges to a separation of linear from nonlinear effects. One may have to resort to off-shore measurements of tides, predict these, and allow for nonlinearity by direct comparison of offshore and onshore tides. Concerning such efforts, it seems appropriate to close with the remarks of Hilaire Belloc (1925) 'When they pontificate on the tides it does no great harm, for the sailorman cares nothing for their theories, but goes by real knowledge.'

This study has been generously supported by the U.S. Coast and Geodetic Survey, and by the National Science Foundation. The Honolulu and Newlyn observations have been made available through the efforts of Mr B. Zetler and Dr J. Rossiter, respectively.

Appendix A. Derivation of input functions

(*a*) *Gravitational potential*

The gravitational potential resulting from a mass M ($\mathbb{C}$ or $\odot$) at a test point $\mathrm{P}(r, \theta, \lambda)$ is $V = GM/\rho$, where G is the gravitational constant, and ρ the distance PM. Expanding in terms of the parallax $\xi = r/R$, we have (figure 13):

$$V = \frac{GM}{\rho} = \frac{GM}{R}[1 - 2\xi\mu + \xi^2]^{-\frac{1}{2}} = \frac{GM}{R}\sum_{n=0}^{\infty}\xi^n P_n(\mu), \tag{A 1}$$

where $\mu = \cos\alpha$, and

$$P_n(\mu) = \frac{1}{2^n n!}\frac{d^n}{d\mu^n}(\mu^2-1)^n$$

are the Legendre polynomials:

$$P_0 = 1, \quad P_1 = \mu, \quad P_2 = \tfrac{3}{2}\mu^2 - \tfrac{1}{2}, \quad P_3 = \tfrac{5}{2}\mu^3 - \tfrac{3}{2}\mu, \quad \ldots.$$

The first term, $n = 0$ is a constant of no interest. The second term, $(GM/R^2)\, r\cos\alpha$, represents a uniform force GM/R^2 in the direction O to M on all points of the Earth; this enters in the Kepler–Newtonian equations for orbital motion and is not part of the tidal effect.

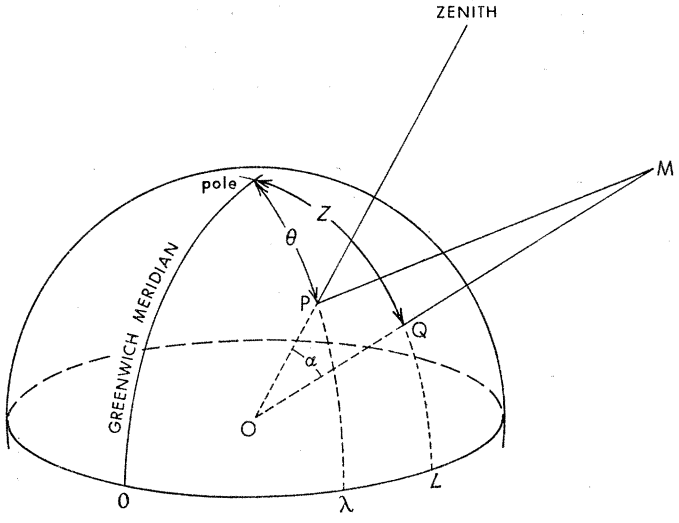

FIGURE 13. α is the zenith angle of M (Moon or Sun) at a point P on the Earth's surface. Z is the polar angle and L the terrestrial east longitude of M. θ, λ are polar angle (colatitude) and longitude of P. r = OP is the distance from the Earth's centre to P, and R = OM the distance to M, ρ = PM the distance from P to M.

Now write $G = ga^2/M_\oplus$ where a is the Earth's radius and $M_\oplus$ its mass. The equilibrium tide can be written

$$\frac{V}{g} = a\frac{M}{M_\oplus}\sum_{n=2,3,\ldots}^{\infty}\xi^{n+1}P_n(\mu) = \sum_{n=2,3,\ldots}^{\infty}K_n\left(\frac{\bar{R}}{R}\right)^{n+1}P_n(\mu), \quad K_n = a\frac{M}{M_\oplus}\bar{\xi}^{n+1}, \tag{A 2}$$

where $\bar{\xi} = (a/\bar{R})$. For the Moon and Sun, $K_2 = 35{\cdot}785$ and $16{\cdot}427$ cm, respectively.† This is the usual formulation (Shureman 1941, p. 119, Doodson‡ 1921, p. 307).

(*b*) *Radiational function*

We define a radiational function

$$\mathscr{R} = S(\bar{R}_\odot/\rho_\odot)\cos\alpha \quad \text{in day-time} \quad (0\leqslant\alpha\leqslant\tfrac{1}{2}\pi),$$

$$0 \quad \text{in night-time} \quad (\tfrac{1}{2}\pi\leqslant\alpha\leqslant\pi),$$

where $S = 1{\cdot}946\,\mathrm{cal\,cm^{-2}\,min^{-1}}$ is the 'solar constant'. Using the expansion for $1/\rho$ as in equation (A 1), the day-time value can be written

$$S(\bar{R}/R)\,\mu\sum_{n=0}^{\infty}P_n(\mu) = S(\bar{R}/R)\,\mu(1+\xi\mu+\ldots) \quad (1\geqslant\mu\geqslant 0) \tag{A 3}$$

† These figures are derived from the estimates quoted by Allen (1963): $M_\oplus/M_\leftmoon = 81{\cdot}33\pm0{\cdot}03$ $M_\odot = 33270M_\oplus$, $a = 6371{\cdot}0$ km. The Moon's and Sun's mean equatorial horizontal parallaxes are $\bar{\xi} = 3422''{\cdot}62$ and $8''{\cdot}79415$, respectively. The ellipticity of the Earth is ignored in this derivation.

‡ Doodson uses $\frac{3}{2}K_2$.

plus terms of order ξ^2 which are negligible ($\xi_\odot = 1/23\,455$). Expanding $\mathscr{R}$ in spherical harmonics, $\mathscr{R} = S(\bar{R}/R)\sum_{n=0}^{\infty}\kappa_n P_n(\mu)$, we find

$$\kappa_0 = \frac{1}{2}\int_0^1 (\mu+\xi\mu^2+\ldots)\,\mathrm{d}\mu = \tfrac{1}{4}+\tfrac{1}{6}\xi+\ldots,$$

$$\kappa_1 = \frac{3}{2}\int_0^1 (\mu+\xi\mu^2+\ldots)\,\mu\,\mathrm{d}\mu = \tfrac{1}{2}+\tfrac{3}{8}\xi,$$

$$\kappa_2 = \frac{5}{2}\int_0^1 (\mu+\xi\mu^2+\ldots)\,(\tfrac{3}{2}\mu^2-\tfrac{1}{2})\,\mathrm{d}\mu = \tfrac{5}{16}+\tfrac{1}{3}\xi+\ldots,$$

etc. For subsequent odd coefficients, the leading terms can be written

$$\kappa_n = \frac{2n+1}{2}\left[\frac{(1)\,(-1)\,(-3)\ldots(4-n)}{(4)\,(6)\ldots(3+n)}\right]\xi \quad (n=3,5,\ldots),$$

and these are of order ξ and can again be ignored. For the even terms

$$\left.\begin{aligned}\mathscr{R} &= S(\bar{R}_\odot/R)\,\{\tfrac{1}{4}+\tfrac{1}{2}\mu+\sum_{n=2,4,\ldots}\kappa_n P_n(\mu)\}\\ \kappa_n &= \frac{2n+1}{2}\left[\frac{(1)\,(-1)\ldots(3-n)}{(2)\,(4)\ldots(2+n)}\right]\ (n=2,4,6,\ldots).\end{aligned}\right\} \tag{A 4}$$

The first term in (A 4) represents the mean radiation, $\mathscr{R}_0 = \frac{1}{4}S$. For the entire surface this equals $\frac{1}{4}S4\pi a^2 = \pi a^2 S$, the cross-section times the mean radiation. The term is balanced by infrared back radiation and enters into the overall heat balance of the planet. The first term in (A 4) plays a role similar to the term $\xi\mu$ in the expression (A 1) for the gravitational potential. These terms represent mean radiation and mean force, respectively, and both can be ignored in the study of tides. An essential distinction is that the radiational function commences with $P_1(\mu) = \mu$, the gravitational potential with $P_2(\mu)$.

(c) *Expansion in Greenwich coordinates*

The expressions (A 2) and (A 4) for the gravitational and radiational functions, respectively, are of the form $\sum_n f_n(\mu, R)$ where μ, R are functions of time. We need to express $\mu(t)$ as a function of the station coordinates θ, λ, and of the Moon's (Sun's) angular coordinates $Z(t)$, $L(t)$. Let

$$U_n^m + \mathrm{i}V_n^m = Y_n^m = (-1)^m\left[\frac{2n+1}{4\pi}\right]^{\frac{1}{2}}\left[\frac{(n-m)!}{(n+m)!}\right]^{\frac{1}{2}} P_n^m(\cos\theta)\,\mathrm{e}^{\mathrm{i}m\lambda} \tag{A 5}$$

designate the (complex) spherical harmonic so normalized (Backus 1958) that

$$\int |Y_n^m|^2 \sin\theta\,\mathrm{d}\theta\,\mathrm{d}\lambda = 1,$$

and

$$P_n^m(\mu) = \frac{(1-\mu^2)^{\frac{1}{2}m}}{2^n n!}\frac{\mathrm{d}^{m+n}}{\mathrm{d}\mu^{m+n}}(\mu^2-1)^n \quad (n\geqslant 0,\ |m|\leqslant n)$$

is the associated Legendre function:†

$$P_0^0 = 1, \qquad P_1^0 = \cos\theta, \qquad P_1^1 = \sin\theta,$$

$$P_2^0 = \tfrac{3}{2}\cos^2\theta - \tfrac{1}{2}, \qquad P_2^1 = 3\sin\theta\cos\theta, \qquad P_2^2 = 3\sin^2\theta,$$

$$P_3^0 = \tfrac{5}{2}\cos^3\theta - \tfrac{3}{2}\cos\theta, \qquad P_3^1 = \tfrac{3}{2}\sin\theta(5\cos^2\theta - 1), \qquad P_3^2 = 15\sin^2\theta\cos\theta, \qquad P_3^3 = 15\sin^3\theta.$$

† This is the normalization used by Morse & Feshbach (1953) and $n!(n-m)!$ times the normalization by Jeffreys & Jeffreys (1950).

For any two points on a sphere, θ_i, λ_i, $i = 1, 2$, the expression

$$\text{sum} = \sum_{m=-n}^{n} Y_n^m(\theta_1, \lambda_1)\, Y_n^{m*}(\theta_2, \lambda_2)$$

depends only on the distance between the two points, and is the same regardless of where the coordinate system is centred. First, centre the coordinate system at the station P ($i=1$) with zero longitude through the sublunar (subsolar) point Q ($i=2$):

$$\text{sum} = \sum_{m=-n}^{n} Y_n^m(0,0)\, Y_n^{m*}(\alpha, 0) = Y_n^0(0)\, Y_n^0(\mu) = \frac{2n+1}{4\pi} P_n(\mu).$$

Next, orient the coordinates in accordance with the Greenwich system

$$\text{sum} = \sum_{m=-n}^{n} Y_n^m(\theta, \lambda)\, Y_n^{m*}(Z, L),$$

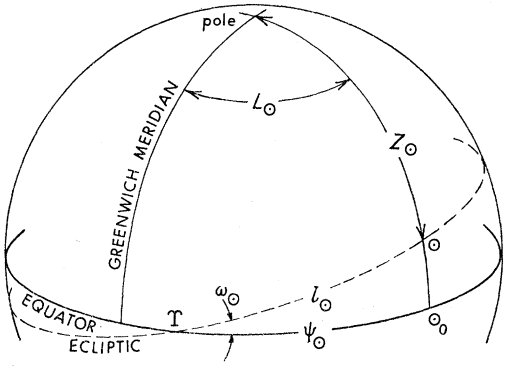

FIGURE 14. Υ is vernal equinox, $\omega_\odot = 23°{\cdot}452$ is abliquity of ecliptic, $l_\odot$ is (instantaneous) longitude of Sun $\odot$ along the ecliptic. $Z_\odot$ is polar angle, $L_\odot$ terrestrial east longitude, $\psi_\odot$ (or $\Upsilon\odot_0$) is the Sun's right ascension.

Equating the two expressions for sum yields

$$P_n(\mu) = \frac{4\pi}{2n+1} \sum_{m=-n}^{n} Y_n^{m*}(Z, L)\, Y_n^m(\theta, \lambda)$$

$$= \frac{4\pi}{2n+1}\left\{U_n^0(Z, L)\, U_n^0(\theta, \lambda) + 2\sum_{m=1}^{m} [U_n^m(Z, L)\, U_n^m(\theta, \lambda) + V_n^m(Z, L)\, V_n^m(\theta, \lambda)]\right\}, \quad \text{(A 6)}$$

where $Y = U + iV$; in equation (A 6) we have avoided negative values of m by use of the identity $Y_n^{-m} = (-1)^m\, Y_n^{m*}$. With this substitution for $P_n(\mu)$ the gravitational function (A 2) or the radiational function (A 4) can be written in the form

$$f_n^m(Z, L; \theta, \lambda) = c_n^m(Z, L)\, Y_n^m(\theta, \lambda) = a_n^m(Z, L)\, U_n^m(\theta, \lambda) + b_n^m(Z, L)\, V_n^m(\theta, \lambda). \quad \text{(A 7)}$$

(*d*) *Solar orbital constants*

We require the polar angle Z, the terrestrial longitude L and the distance R of Sun or Moon in terms of the orbital parameters. From triangle $\Upsilon\odot\odot_0$ (figure 14) we have

$$\cos Z_\odot = \sin l_\odot \sin \omega_\odot, \quad \text{(A 8)}$$

$$\tan \tfrac{1}{2}\psi_\odot = \frac{\sin \tfrac{1}{2}(90° + \omega_\odot)}{\sin \tfrac{1}{2}(90° - \omega_\odot)} \tan \tfrac{1}{2}(l_\odot + Z_\odot - 90°), \quad \text{(A 9)}$$

where $\omega_\odot = 23°{\cdot}452$ is the obliquity of the ecliptic, and $l_\odot$ is the instantaneous longitude (in the ecliptic). By Kepler's laws,

$$l_\odot = h_\odot + 2e_\odot \sin(h_\odot - p_\odot) + \tfrac{5}{4} e_\odot^2 \sin 2(h_\odot - p_\odot) + \ldots, \tag{A 10}$$

where $h_\odot$ is the mean longitude, $p_\odot$ the longitude of perigee and $e_\odot$ the eccentricity of the orbit.

The right ascension of Greenwich is given by

$$\psi_G = 15°(t - 12^h) + h_\odot. \tag{A 11}$$

Then

$$L_\odot = \psi_\odot - \psi_G \tag{A 12}$$

is the longitude east of Greenwich of the Sun's meridian. The terms $c_n^m(Z, L)$ vary with $L_\odot$ as $\exp(imL_\odot)$, where $mL_\odot = m\,15°\,t^h$ plus slowly varying terms, so that the argument increases by 360° in approximately $(360°/15°m)$ h. Accordingly we refer to $m = 0, 1, 2, \ldots$ as the long period, diurnal, semidiurnal, ..., tides, respectively.

Finally, the distance $R_\odot$ between Sun and Earth is related to the eccentricity $e_\odot$ and the mean anomoly $h_\odot - p_\odot$ by the law for an elliptical orbit:

$$\bar{R}_\odot / R_\odot = 1 + e_\odot \cos(h_\odot - p_\odot) + e_\odot^2 \cos 2(h_\odot - p_\odot) + \ldots, \tag{A 13}$$

where $\bar{R}_\odot \propto 1/(\text{mean equatorial parallax})$, not the Sun's mean distance. Equations (8), (12) and (13) determine $Z_\odot$, $L_\odot$ and $R_\odot$ in terms of $h_\odot$, $p_\odot$ and $e_\odot$. When these are substituted into (A 7) and (A 2), and the resulting expressions expanded in powers of small parameters (the ellipticity, obliquity and parallax), we obtain the classical line spectrum of frequencies f_k (equation (2·2)).

It remains to express $h_\odot$, $p_\odot$ and $e_\odot$ as functions of time. Let t designate Greenwich time in hours since 1 January 1900 at 0 hours G.C.T. Then

$$T = \frac{t + 12^h}{(24)\,(36525)} \tag{A 14}$$

is the time in Julian centuries since noon, 31 December 1899, as used in most astronomical texts. The Sun's mean longitude, and the longitude of perigee (both in radians) are given by

$$\left.\begin{aligned} h_\odot &= 4{\cdot}8816280 + 628{\cdot}3319509\,T + 0{\cdot}0000052\,T^2, \\ p_\odot &= 4{\cdot}9082295 + 0{\cdot}0300053\,T + 0{\cdot}0000079\,T^2, \end{aligned}\right\} \tag{A 15}$$

respectively. The eccentricity is taken by Doodson as constant, $e_\odot = 0{\cdot}0167504$. A somewhat more accurate expression is

$$e_\odot = 0{\cdot}01675104 - 0{\cdot}00004180\,T - 0{\cdot}000000126\,T^2. \tag{A 16}$$

(e) *Lunar orbital constants*

Here the situation is more complicated. The mean longitude $h_\mathbb{C}(T)$, longitude of perigee $p_\mathbb{C}(T)$ and of the node $n_\mathbb{C}(T)$ (all along the ecliptic) are given by

$$\left.\begin{aligned} h_\mathbb{C} &= 4{\cdot}7200089 + 8399{\cdot}7092745\,T + 0{\cdot}0000346\,T^2, \\ p_\mathbb{C} &= 5{\cdot}8351526 + \quad 71{\cdot}0180412\,T - 0{\cdot}0001801\,T^2, \\ n_\mathbb{C} &= 4{\cdot}5236016 - \quad 33{\cdot}7571463\,T + 0{\cdot}0000363\,T^3. \end{aligned}\right\} \tag{A 17}$$

Solving the triangle $\Upsilon A\Omega$ with sides ν, $A\Omega$, $n_{\leftmoon}$ we have

$$\cos\omega_{\leftmoon} = \cos\omega_{\odot}\cos i - \sin\omega_{\odot}\sin i\cos n_{\leftmoon},$$

$$\sin\nu = \sin i\sin n_{\leftmoon}/\sin\omega,$$

$$\sin A\Omega = \sin n_{\leftmoon}\sin\omega_{\odot}/\sin\omega_{\leftmoon},$$

$$\cos A\Omega = \cos n_{\leftmoon}\cos\nu + \cos\omega_{\odot}\sin n_{\leftmoon}\sin\nu,$$

$$\tan\tfrac{1}{2}A\Omega = \sin A\Omega/(1+\cos A\Omega).$$

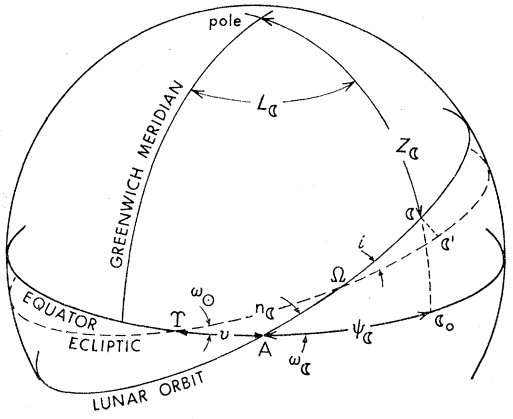

FIGURE 15. Υ is vernal equinox. $n_{\leftmoon} = \Upsilon\Omega$ is longitude (along ecliptic) of ascending node reckoned from equinox. $\omega_{\odot} = 23°{\cdot}452$ is obliquity of ecliptic, $i = 5°{\cdot}145$ is inclination of Moon's orbit to ecliptic. $l_{\leftmoon} = A\leftmoon$, is (instantaneous) longitude of Moon $\leftmoon$, along its orbit. $Z_{\leftmoon}$ is polar angle, $L_{\leftmoon}$ is terrestrial east longitude, and $\Upsilon\leftmoon_0$ the Moon's right ascension.

The mean longitude of the Moon in its orbit is

$$\sigma_{\leftmoon} = h_{\leftmoon} - n_{\leftmoon} + A\Omega$$

and the (instantaneous) longitude $A_{\leftmoon}$ in its orbit equals†

$$\begin{aligned} l_{\leftmoon} = {} & \sigma_{\leftmoon} + 2e_{\leftmoon}\sin(h_{\leftmoon} - p_{\leftmoon}) + \tfrac{5}{4}e_{\leftmoon}^2\sin 2(h_{\leftmoon} - p_{\leftmoon}) \\ & + me_{\leftmoon}(\tfrac{15}{4} + \tfrac{263}{16}m)\sin(h_{\leftmoon} - 2h_{\odot} + p_{\leftmoon}) + m^2(\tfrac{11}{8} + \tfrac{59}{12}m + \tfrac{75}{16}e_{\leftmoon}^2/m)\sin 2(h_{\leftmoon} - h_{\odot}) \\ & + \tfrac{17}{8}m^2e_{\leftmoon}\sin(3h_{\leftmoon} - 2h_{\odot} - p_{\leftmoon}) + \tfrac{77}{16}m^2e_{\odot}\sin(2h_{\leftmoon} - 3h_{\odot} + p_{\odot}), \end{aligned} \tag{A 18}$$

where $e_{\leftmoon} = 0{\cdot}054900$ is the eccentricity of the Moon's orbit, and $m = 0{\cdot}074804$ the ratio of mean motions of $\odot$ to $\leftmoon$. The Moon's distance is given by†

$$\begin{aligned} \bar{R}_{\leftmoon}/R_{\leftmoon} = {} & 1 + (1+\tfrac{1}{6}m^2)^{-1}[e_{\leftmoon}\cos(h_{\leftmoon} - p_{\leftmoon}) + e_{\leftmoon}^2\cos 2(h_{\leftmoon} - p_{\leftmoon}) \\ & + me_{\leftmoon}(\tfrac{15}{8} + \tfrac{329}{64}m)\cos(h_{\leftmoon} - 2h_{\odot} + p_{\leftmoon}) + m^2(1 + \tfrac{19}{6}m + \tfrac{15}{4}e_{\leftmoon}^2/m)\cos 2(h_{\leftmoon} - h_{\odot}) \\ & + \tfrac{33}{16}m^2e_{\leftmoon}\cos(3h_{\leftmoon} - 2h_{\odot} - p_{\leftmoon}) + \tfrac{7}{2}m^2e_{\odot}\cos(2h_{\leftmoon} - 3h_{\odot} + p_{\odot})]. \end{aligned} \tag{A 19}$$

† The usual formulae are correct to second order in e and m. However, some of the third-order terms, given completely in Smart (1953, pp. 281–285), are of the same numerical order of magnitude as the smaller second-order terms, and may be important when $n = 2$ or greater. To include all the third-order terms would involve 6 extra trigonometrical factors in each equation, and this seems hardly justified. By judicious selection, the following equations each contain only two extra trigonometric factors, and reduce the magnitudes of the largest neglected terms from 0·0050 to 0·0005 in $l_{\leftmoon}$, and from 0·0016 to 0·0002 in $R_{\leftmoon}/R_{\leftmoon}$.

The polar distance $Z_{\leftmoon}$ is given by

$$\cos Z_{\leftmoon} = \sin l_{\leftmoon} \sin \omega_{\leftmoon} \quad (0 < Z_{\leftmoon} < \pi). \tag{A 20}$$

Also,
$$\tan \tfrac{1}{2}\psi_{\leftmoon} = \frac{\sin \tfrac{1}{2}(90^\circ + \omega_{\leftmoon})}{\sin \tfrac{1}{2}(90^\circ - \omega_{\leftmoon})} \tan \tfrac{1}{2}(l_{\leftmoon} + Z_{\leftmoon} - 90^\circ)$$

with $0 < \frac{1}{2}\psi_{\leftmoon} < \pi$. The Moon's right ascension is then $\Upsilon\!\!\leftmoon_0 = \nu + \psi_{\leftmoon}$, and its longitude east of Greenwich is

$$L_{\leftmoon} = \nu + \psi_{\leftmoon} - \psi_G. \tag{A 21}$$

Appendix B. Sampling distributions and confidence limits

We refer to the complex spectrum estimators G_r, H_r (§ 4 (*b*)) at a particular frequency $(r/355)$ c/d, and consider ensemble averages of their product from analysis of p independent segments of the time series. From equation (4·8) we obtain as estimate of the admittance Z,

$$\tilde{Z} = \tilde{X} + \mathrm{i}\tilde{Y} = \langle G_r H_r^* \rangle / \langle G_r G_r^* \rangle = Z + \epsilon$$

where the sampling error is $\epsilon = \langle |N_r|\, |G_r|\, \mathrm{e}^{-\mathrm{i}\nu_r} \rangle / \langle |G_r|^2 \rangle$. (B 1)

The input energy $|G_r|^2$ is by definition noise-free and approximately constant from sample to sample, and the relative phase ν_r has uniform expectation in $(0, 2\pi)$. Therefore the real and imaginary parts of (B 1) have approximately normal independent probability distributions, each with mean value zero, and variance given by

$$\sigma'^2 = (2p)^{-1} \sigma_N^2 / \sigma_G^2 = (2p)^{-1} R^2 (\gamma^{-2} - 1), \tag{B 2}$$

where σ_N^2 and σ_G^2 are the long-term average variances of noise and input signal respectively, $R^2 = X^2 + Y^2 = |Z|^2$, and γ^2 is the true coherence. This result differs from the more difficult case analysed by Goodman (1957), in which $|G_r|$ has a Rayleigh distribution appropriate to a random input.

$\tilde{X}$ and $\tilde{Y}$ are thus unbiased, independent estimates of X and Y, with the joint probability distribution

$$p(\tilde{X}, \tilde{Y}) = (2\pi\sigma'^2)^{-1} \exp\left[-\{(\tilde{X} - X)^2 + (\tilde{Y} - Y)^2\}/2\sigma'^2\right]. \tag{B 3}$$

The distributions of $\tilde{R} = \sqrt{(\tilde{X}^2 + \tilde{Y}^2)}$ and $\tilde{\theta} = \arctan(\tilde{X}/\tilde{Y})$ are derived by transforming (B 3) to the variables $(\tilde{R}, \tilde{\theta})$ and integrating with respect to $\tilde{\theta}$ and $\tilde{R}$ respectively. With normalized variables,

$$\rho = \tilde{R}/R, \quad \theta = \tilde{\theta} - \text{true phase lead}, \quad \sigma = \sigma'/R,$$

the results are
$$p(\rho) = (\rho/\sigma^2) \exp\left[-(\rho - 1)^2/2\sigma^2\right] \quad [e^{-\rho/\sigma^2} I_0(\rho/\sigma^2)], \tag{B 4}$$

$$p(\theta) = (2\pi)^{-1} \exp(-1/2\sigma^2)\, [1 + F(\cos\theta/\sigma)], \tag{B 5}$$

where $I_0(x)$ is a modified Bessel Function, and

$$F(x) = x \mathrm{e}^{\frac{1}{2}x^2} \int_{-x}^{\infty} \mathrm{e}^{-\frac{1}{2}t^2}\, \mathrm{d}t.$$

The functions defined by (B 4) and (B 5) have been computed, and are represented in the top half of figure (16) for $\sigma = 0{\cdot}1$, $0{\cdot}2$, $0{\cdot}4$, $0{\cdot}6$, $0{\cdot}8$ and $1{\cdot}0$. For values of $\sigma > 1{\cdot}0$ the distributions are too broad to be of any practical use. For values of $\sigma < 0{\cdot}1$, both $p(\rho)$ and $p(\theta)$ approximate to normal distributions with variance σ^2.

It is seen that the distribution of θ is always symmetrical about $\theta = 0$ (i.e. $\tilde{\theta}$ is an unbiased estimator of θ), but the distribution of ρ is biased positively (i.e. $\tilde{R}$ tends to be somewhat greater than R). The mean or 'expected' value of ρ is found to be

$$(\tfrac{1}{2}\pi)^{\frac{1}{2}}\sigma_1 F_1(-\tfrac{1}{2}; 1; -\sigma), \tag{B 6}$$

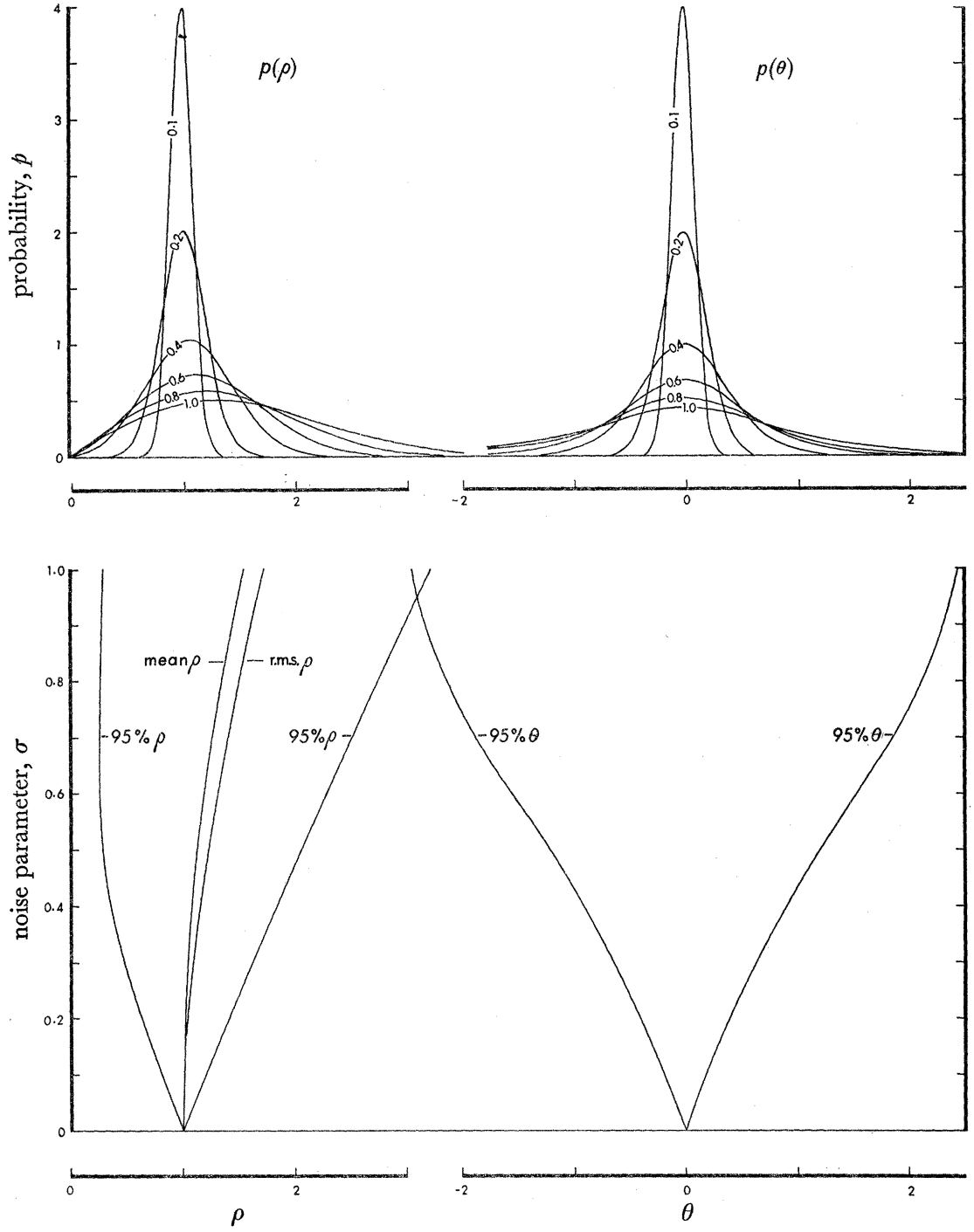

FIGURE 16. The upper diagrams show the probability distributions of (left) ρ = sample admittance/true admittance, and (right) θ = sample phase − true phase, for stated values of the noise parameter $\sigma = [(\gamma^{-2}-1)/2p]^{\frac{1}{2}}$ where γ^2 is the coherence, and p the degrees of freedom. The lower diagrams show the 95 % confidence limits of the same quantities, and also the mean and r.m.s. values of ρ, all plotted against σ.

where ${}_1F_1(a;\, b;\, x)$ is Kummer's hypergeometric function (tabulated in Slater 1960). However, its r.m.s. value is simply

$$(1+2\sigma^2)^{\frac{1}{2}}. \tag{B 7}$$

Both (B 6) and (B 7) are represented in the lower left-hand part of figure (16). The 95 % confidence limits of ρ and θ, defined such that 0·025 of the distribution lies to the left of the lower, and 0·025 to the right of the upper limit, computed by quadrature, are also plotted.

The sampling distribution of the coherence estimate, $\tilde{\gamma}^2 = |G_r H_r^*|^2/(|G_r|\,|H_r|)^2$, is much more complicated, even with constant $|G_r|$. We have

$$\begin{aligned}\tilde{\gamma}^2 &= [(X+\epsilon_1)^2+(Y+\epsilon_2)^2]/[(X+\epsilon_1)^2+(Y+\epsilon_2)^2+\epsilon_3^2-\epsilon_1^2-\epsilon_2^2] \\ &= 1-(\epsilon_3^2-\epsilon_1^2-\epsilon_2^2)/(R^2+2\epsilon_1 X+2\epsilon_2 Y+\epsilon_3^2),\end{aligned} \tag{B 8}$$

where

$$\epsilon_1+i\epsilon_2 = \epsilon \quad \text{and} \quad \epsilon_3^2 = \langle|N_r|^2\rangle|\langle|G_r|^2\rangle. \tag{B 9}$$

With $p = 1$, (i.e. no ensemble averaging), comparison of (B 1) and (B 9) shows that $\epsilon_3^2 = \epsilon_1^2+\epsilon_2^2$, so that $\tilde{\gamma}^2 = 1$ identically. With $p > 1$, it can be shown that $\tilde{\gamma}^2 < 1$, but $\tilde{\gamma}^2-\gamma^2$ is still biased positively by an amount which decreases with increasing p. We make the simplifying approximation that the 'expected' value of $\tilde{\gamma}^2$, say $E(\tilde{\gamma}^2)$, is the same as the right side of (B 8) with numerator and denominator each put equal to its own 'expected' value. A little algebra then gives

$$E(\tilde{\gamma}^2) \doteqdot \gamma^2+p^{-1}(1-\gamma^2).$$

Values of $E(\tilde{\gamma}^2)$ so defined compare reasonably well with exact mean values of the distributions for Goodman's case of random input, computed and tabulated by Amos & Koopmans (1963). An approximately unbiased estimate of the true coherence γ^2 is therefore

$$(p\tilde{\gamma}^2-1)/(p-1) \quad (p>1). \tag{B 10}$$

The expression (B 10) is negative if $\tilde{\gamma}^2 < p^{-1}$, but in such a case the true coherence (fundamentally positive) is probably too small to be of interest.

To obtain the confidence limits shown in figure 1, etc., we used the unbiased estimate of γ^2 from (B 10) to form the normalized parameter $\sigma^2 = (2p)^{-1}(\gamma^{-2}-1)$, and thence the normalized confidence limits for ρ and θ. The limits for R and θ are then obtained from $\tilde{R}$ and $\tilde{\theta}$ by dividing by or subtracting, respectively, the normalized limits. The limits for X and Y are simply $\tilde{X}\pm 1{\cdot}96\sigma'$, $\tilde{Y}\pm 1{\cdot}96\sigma'$, from (B 2).

Although the above results are derived strictly for a fixed frequency r, which implies $|G_r|$ is nearly constant, they may be shown to be approximately valid for ensemble averages over adjacent values of r also.

Appendix C. Horn folding

Suppose the tide record is sampled some fixed time t h following the meridian passage of the mean Moon. A plot of such points varies slowly with time, with frequencies up to a few cycles per month. The spectrum $H_0(f)$ of these discrete points can be related to the spectrum $H(f)$ of the continuous record, $\zeta(t)$, as follows: daily sampling is equivalent to multiplying $\zeta(t)$ with a 'Dirac Comb' of delta functions,

$$D(t) = \delta(t)+\delta(t+24\,\text{lunar hours})+\delta(t+48\,\text{lh})+\ldots.$$

According to the convolution theorem, the spectrum of the discrete record $\zeta(t)\,D(t)$ is given by

$$H_0(f) = H(f)+H(q-f)+H(q+f)+H(2q-f)+\ldots,$$

where q is the sampling frequency, once per lunar day. It is as if $H(f)$ were folded in accordian fashion, with the frequencies $M_1, M_2, M_3, M_4, \ldots$, all overlapping with zero frequency. An analysis of the once-daily points for $(0\ k_2'\ k_3'\ k_4'\ k_5'\ k_6')$ of species 0 includes the effects of $(k_1\ +k_2'\ +k_3'\ +k_4'\ +k_5'\ +k_6')$ and $(k_1\ -k_2'\ -k_3'\ -k_4'\ -k_5'\ -k_6')$ of species $k_1 = 1, 2, \ldots$ in the continuous record. Horn uses 44 frequencies, starting from zero frequency (0 0 0 0 0) and the nodal frequency (0 0 0 0 1) to 4 c/m (0 4 −4 0 0). This gives a satisfactory prediction for t lunar hours, with no need for f, u-factors. To predict the complete marigram, the analysis is repeated for each hour t, thus yielding 24×44 amplitudes and phases. In a similar manner, Horn analyses and predicts the times and heights of the four daily extremes. The method has some obvious advantages when limitations imposed by analogue analysers restricts the number of constituents which can be evaluated at one time, or if the prediction can be limited to extremes.

References

Allen, C. W. 1963 *Astrophysical quantities*. University of London Press.

Amos, D. E. & Koopmans, L. H. 1963 Sandia Corp. Monograph, SCR 483.

Backus, G. 1958 *Ann. Phys.* **4**, 372–447.

Belloc, H. 1925 *The cruise of the Nona*. London: Constable.

Cartwright, D. E. & Catton, D. B. 1963 *Int. Hydr. Rev.* **40**, 1, 113–125.

Doodson, A. T. 1921 *Proc. Roy Soc.* A, **100**, 305–329.

Doodson, A. T. 1947 *Int. Hydr. Rev.* **24**.

Goodman, N. R. 1957 *Tech. Rep. no.* 8. College of Engineering, New York University.

Haubrich, R. A. & Munk, W. H. 1959 *J. Geophys. Res.* **64**, 2373–2388.

Horn, W. 1948 *Dtsch. Hydr. Z.* **1**, 124–140.

Horn, W. 1960 *Int. Hydr. Rev.* **37**, 65–94.

Jeffreys, H. & Jeffreys, B. 1950 *Methods of mathematical physics*. Cambridge University Press.

Lamb, H. 1932 *Hydrodynamics*, Cambridge University Press.

Longuet-Higgins, M. S. 1965 Symons Memorial Lecture. *Quart. J. R. Met. Soc.* **91**, 425–451.

Morse, P. M. & Feshbach, H. 1953 *Methods of theoretical physics*. New York: McGraw-Hill.

Munk, W. H. & Bullard, E. C. 1963 *J. Geophys. Res.* **68**, 3627–3634.

Munk, W. H. & Hasselmann, K. F. 1964 *Studies on oceanography* (Hidaka Volume) (Tokyo), pp. 339–344.

Munk, W. H. 1960 *J. Meteor.* **17**, 92–93.

Munk, W. H., Zetler, B. & Groves, G. W. 1965 *Geophys. J.* **10**, 211–219.

Pattullo, J., Munk, W., Revelle, R. & Strong, E. 1955 *J. Mar. Res.* **14**, 88–155.

Shureman, P. 1941 *Manual of harmonic analysis and prediction of tides*. Washington: U.S. Govt. Printing Office.

Slater, L. J. 1960 *Confluent hypergeometric functions*. Cambridge University Press.

Smart, W. M. 1953 *Celestial mechanics*. London: Longmans, Green and Co.

Snodgrass, F. E. 1964 *Science*, **146**, 198–208.

Whewell, W. 1837 *History of the inductive sciences*, p. 248.